Astron. Astrophys. 334, 873–894 (1998)

ASTRONOMY AND ASTROPHYSICS

Optical and X-ray monitoring, Doppler imaging, and space motion of the young star Par 1724 in Orion⋆,⋆⋆,⋆⋆⋆

R. Neuhäuser[1], S.J. Wolk[2], G. Torres[2], Th. Preibisch[3], N.M. Stout-Batalha[4,†], A.P. Hatzes[5], S. Frink[6], R. Wichmann[7], E. Covino[8], J.M. Alcalá[8], W. Brandner[9], F.M. Walter[10], M.F. Sterzik[1], and R. Köhler[11]

[1] Max-Planck-Institut für Extraterrestrische Physik, D-85740 Garching, Germany (rne@mpe.mpg.de)
[2] Center for Astrophysics, 60 Garden Street, Cambridge, MA 02138, USA
[3] Astronomisches Institut, Universität Würzburg, Am Hubland, D-97074 Würzburg, Germany
[4] Lick Observatory, University of California, Santa Cruz, CA 95064, USA
[5] Astronomy Department, University of Texas, Austin, TX 78712, USA
[6] Astronomisches Rechen-Institut Heidelberg, Mönchhofstraße 12-14, D-69120 Heidelberg, Germany
[7] IUCAA, Post Bag 4, Ganeshkhind, Pune 411007, India
[8] Osservatorio Astronomico di Capodimonte, I-80131 Napoli, Italy
[9] Caltech - JPL/IPAC, Mail Code 100-22, Pasadena, CA 91125, USA
[10] Department of Physics and Astronomy, SUNY, Stony Brook, NY 11794-3800, USA
[11] Astrophysikalisches Institut Potsdam, An der Sternwarte 16, D-14482 Potsdam, Germany

Received 8 December 1997 / Accepted 23 February 1998

Abstract. We present a detailed study of the young T Tauri star Par 1724, located 15 arc min north of the Trapezium cluster in Orion. Our extensive VRI photometric measurements confirm the rotational period to be 5.7 days. Repeated high-resolution spectra show variability in the radial velocity with the same period. A Doppler imaging analysis based on high-S/N high-resolution spectra yields an image showing a pronounced dark feature (spot) at relatively low latitude, which is responsible for most or all of the observed variability. Our high-resolution spectra yield a rotational velocity of $v \cdot \sin i \simeq 71\ km\ s^{-1}$, a surface gravity of $\log g \simeq 3$, and a mean heliocentric radial velocity of $\sim 23\ km\ s^{-1}$, the latter being consistent with membership to the Orion association. The equivalent width of the lithium 6708Å line is variable, consistent with rotational modulation. The line is stronger when the spot is on the front side; the lithium abundance observed when the spot is on the back side is consistent with the primordial value. Many ROSAT X-ray observations show that Par 1724 is a strong and variable X-ray source. It has shown one of the most powerful X-ray flares. Our deep infrared imaging at high spatial resolution reveals no physically bound visual companions down to ~ 1 arc sec separations and a magnitude difference up to $\Delta R = 7$ mag, and also no companion down to ~ 0.13 arc sec with $\Delta K = 2.5$ mag. We also present the spectral energy distribution of Par 1724 and show that it does not display infrared excess. We estimate the bolometric luminosity to be $\sim 49\ L_\odot$, the spectral type to be K0, and the radius to be $\sim 9\ R_\odot$. Although Par 1724 appears to have lost all its circumstellar material, its bolometric luminosity places it very close to the stellar birth-line at an age of only $\sim 2 \cdot 10^5$ years, with a mass of $\sim 3\ M_\odot$. According to its present location and 3D space motion ($\sim 20\ km\ s^{-1}$ to the north relative to the cluster), Par 1724 may have been ejected from the Trapezium $\sim 10^5$ yrs ago. We cannot rule out that a close companion is responsible for part of the radial velocity variation, but such a close pair might still have been ejected together depending on the encounter dynamics. Par 1724 appears to be a very young, weak-line run-away T Tauri star moving north relative to the Trapezium, but sharing the Orion radial velocity.

Key words: stars: activity – stars: formation – stars: kinematics – stars: pre-main sequence – stars: individual: Par 1724

1. Introduction

Parenago (1954) listed object number 1724, now called Par 1724 or simply P1724, as a relatively bright ($V \simeq 10.6$ mag) star located at $\alpha_{2000} = 5^{\rm h}35^{\rm m}4\overset{\rm s}{.}21$ and $\delta_{2000} = -5°8'13\overset{''}{.}2$, i.e. only $15'$ north of the Trapezium cluster in Orion. It has recently received the variable star designation V1321 Ori (Kazarovets & Samus 1997). Other designations include GSC 4774 0910, Brun 490 (Brun 1934), JW 238 (Jones & Walker 1988), and Strand

Send offprint requests to: Ralph Neuhäuser

⋆ Partly based on observations with the Multiple Mirror Telescope, a joint facility of the Smithsonian Institution and the University of Arizona; the 2.1m telescope at McDonald Observatory; the European Southern Observatory 3.6m, 1.52m, and 0.91m telescopes under programs 57.E-0250, 57.E-0646, and 56.E-0601; the Calar Alto Observatory 3.5m, 2.2m, and 1.2m telescopes; and the Cerro Tololo Inter-American and Kitt Peak National Observatories, NOAO, which are operated by the Association of Universities for Research in Astronomy, under contract with the National Science Foundation.

⋆⋆ Figs. 2, 7, and 10 are available by ftp from CDS.

⋆⋆⋆ Figs. 2,7, and 10 are only available in the online-version of this paper

† Now at: Dep. Astrofisica, Obs. National, Rio de Janeiro, Brasil

51 (Strand 1958); throughout this paper we use P1724, the most common designation for the star. P1724 is listed in the Herbig & Bell (1988) catalog (HBC 452) as a T Tauri star (TTS) with spectral type G8, displaying $H\alpha$ in emission and strong lithium 6708Å absorption.

P1724 appears to be one of the most active TTS known. It has shown one of the most powerful X-ray flares seen on a pre–main sequence star (Gagné et al. 1995; Preibisch, Neuhäuser, & Alcalá 1995).

Tagliaferri et al. (1994) studied the star in considerable detail. From their high-resolution spectra they found no indications of (spectroscopic) multiplicity. They estimated the projected rotational velocity to be $v \cdot \sin i \approx 75\ km\ s^{-1}$, and determined a lithium abundance of $\log\ N$(Li)≈ 3.6, suggesting a very young age. Tagliaferri et al. (1994) classified the star as a classical TTS (cTTS).

Preibisch et al. (1995) recently studied P1724 optically also. They estimated the spectral type to be about K3 and presented a low-resolution spectrum showing $W_\lambda(H\alpha) = 4$Å and W_λ(Li)$= 0.47$Å. Hence, P1724 is more properly classified as a *weak-line* TTS (wTTS).

The X-ray variability of P1724 was studied by Preibisch et al. (1995) and Neuhäuser et al. (1995b). Assuming that it is located in Orion at a distance of $\sim 500\,pc$, Preibisch et al. (1995) observed the largest flare (in terms of total radiated energy) ever reported on a star (surpassed since then; cf. Grosso et al. 1997). If P1724 is actually foreground to Orion, the flare would still be exceptional (cf. Montmerle et al. 1983, Preibisch et al. 1993, Gagné et al. 1995, Kürster & Schmitt 1996).

TTS tend to cluster in dark clouds and form T associations. There are star forming regions (SFR) where it seems that only low-mass stars form (e.g. Taurus–Auriga), as well as others with both low- and high-mass stars such as the Orion OB association, at a distance of $\sim 460\,pc$ (Genzel & Stutski 1989, Brown et al. 1994). Most stars in a T association share the same kinematics, i.e. radial velocity and proper motion. There have been several studies of the proper motion of P1724, and the probability of membership to the Orion association as estimated by different authors ranges from $0\ \%$ to $97\ \%$ (cf. Sect. 9).

One of our goals in this paper is to understand why P1724 shows the extreme behavior in X-rays mentioned above. Due to its possibly peculiar space motion, it may also provide supporting evidence for the hypothesis that low-mass pre-main sequence (PMS) stars can escape from multiple protostellar systems (or dense clusters) and become run-away T Tauri stars. One such star, possibly ejected from the Trapezium, has been presented by Marschall & Mathieu (1988): P1540, a double-lined spectroscopic binary, shows radial velocity consistent with membership to Orion, but its proper motion is different and points away from the Trapezium cluster, from which it might have been ejected $\sim 10^5$ years ago. P1724 may be similar to this star in many respects.

Our paper is organized as follows: In Sect. 2, we discuss the photometry to check the rotational period of P1724. In Sect. 3, we present high-resolution spectra used to monitor the radial velocity and determine the physical parameters of the star. Then, in Sect. 4, we investigate the long-term photometric variations over ~ 30 years and compare it to our recent data on photometric and radial velocity variations, presumably related to spot activity. The spectral energy distribution is presented in Sect. 5, leading to estimates of the mass, radius, and luminosity. Additional high-resolution spectroscopy is described in Sect. 6, and used for reconstruction of the surface temperature distribution by Doppler imaging techniques. We discuss some activity and/or youth indicators in P1724 (Hα, Ca II H & K, and lithium) in Sect. 7, as well as X-ray observations in Sect. 8. The space motion of P1724 is studied in Sect. 9. In Sect. 10, we present R- and K-band imaging and discuss the multiplicity of the star. Finally, we summarize our findings and conclude in Sect. 11.

2. Photometry: the rotational period

Photometric variability in P1724 was first reported by Cutispoto et al. (1996)[1], based on a total of eleven $UBVRI$ observations obtained over a period of 13 nights. They estimated the amplitude of the variations in the V band to be ~ 0.2 mag with a period of 5.6 ± 0.21 days interpreted as due to rotational modulation by spots. Although the Cutispoto et al. light curve appears regular and well-defined, their observations do not allow one to rule out completely the possibility that the true, shorter period has been missed due to undersampling. It is sometimes found that this is the case when much finer sampling is subsequently obtained (e.g., Bouvier et al. 1993).

To investigate this possibility, we monitored P1724 extensively for six weeks with several photometric observations per night in order not to miss possibly very short periods. The star was observed using the 14″ Schmidt-Cassegrain telescope located on the roof of the *Department of Earth and Space Sciences* building at the State University of New York at Stony Brook. The 'Mount Stony Brook' (MTSB) telescope is equipped with a thermoelectrically cooled SBIG ST-6 CCD (cf. Wolk 1996 for more information). Observations were made on 17 nights between 20 Sep 1995 and 11 Nov 1995. In total, 68 observations were made in each of the Johnson V, R, and I filters, four per night.

Additional data were taken from CTIO using the 0.9m telescope, between 30 Jan and 3 Feb 1996. The same field was observed a total of fifteen times in each filter. While the CTIO data had coarse temporal coverage, they had much higher S/N. We also expected that by comparing the results from the independent data sets our conclusions would be strengthened.

Three field stars were used for comparison in both cases. After the data were debiased and flat fielded, fluxes within a $6''$ ($4''$ for CTIO) radius of P1724 and the three comparison stars were summed. An annulus with an inner radius of $7''$ and an outer radius of $10''$ was used for background subtraction. The star JW 242, located four arc sec south of P1724, is fainter than P1724 by several magnitudes (see Sect. 10), and therefore it does not influence the photometry.

[1] Warren & Hesser (1977) had observed the star previously, but did not recognize any variations (however, see Sect. 4).

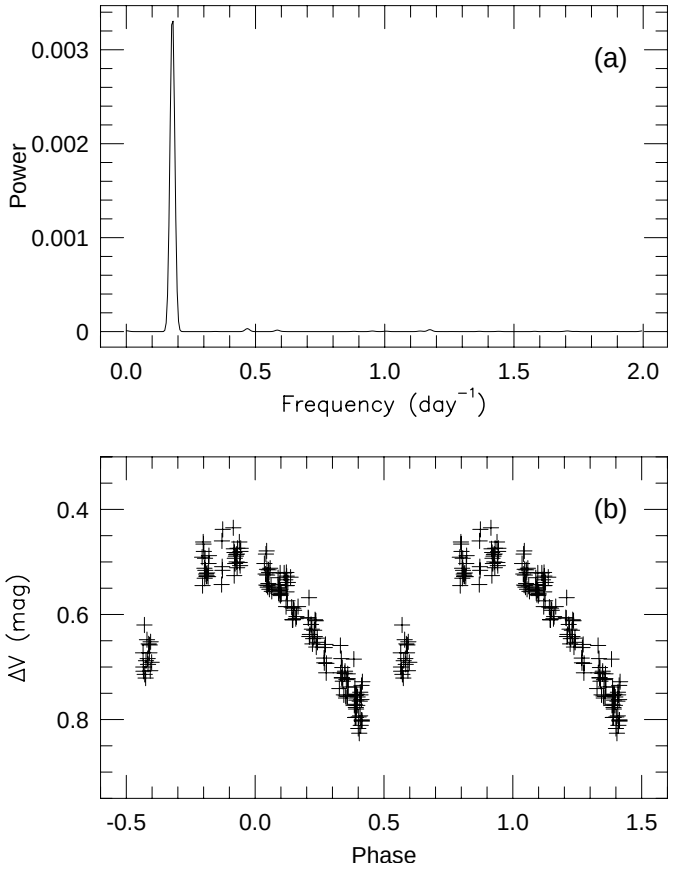

Fig. 1a and b. V-band variation of P1724. **a** Cleaned power spectrum showing one peak with a period of ~ 5.7 days, power units are arbitrary. **b** V-band observations of MTSB folded with the 5.7-day period starting at the epoch of maximum brightness (see text)

Two independent numerical period searching routines were used: a phase dispersion minimization method (Stellingwerf 1978) and a fast Lomb periodogram (Press & Rybicki 1989). The period searches returned three main periods: 0.85 days, 1.21 days, and 5.7 days. Other weaker peaks in the power spectrum are artifacts due to the window function. In order to assess the reality of each of these periods, we experimented by fitting a variety of functions to the data and examining the fits for any residual trends during each night. The 1.2-day periodicity is easily ruled out in this way, but the situation is more ambiguous with the other two. We then applied the CLEAN algorithm (Roberts et al. 1987), which is very effective in discriminating real peaks from aliases in the power spectrum. The result in the V band for the MTSB data set is shown in Fig. 1a, where the single peak corresponds to a period of about 5.7 days. The formal false alarm probability is below 1 %. Thus, the result of Cutispoto et al. (1996) is confirmed. Phased MTSB V-band data are shown in Fig. 1b.

To produce our best estimate of the rotational period we combined the MTSB and CTIO data sets. We fitted sine curves with a fixed offset and amplitude independently to the V, R, and I curves, and iterated on the phase shift and period until the residuals were minimized. Although the light curve is probably not strictly sinusoidal, inspection of the fits revealed that a sine curve is a sufficiently good approximation for our purposes. In all passbands the result is similar, and the average period is $P = 5.6793 \pm 0.0002$ days, with the first maximum occurring at JD 2449984.828. The formal uncertainty in the period is probably an underestimate, due to shortcomings in the model and the very nature of the variation, which is not likely to be strictly periodic. We discuss this in more detail in Sect. 4.

Aside from the MTSB and CTIO observations, one of us (RW) obtained additional photometry in the V and $R_{\rm C}$ (Cousins R) bands at three different sites; we refer to this as the *RW* data set. In Dec 1995 observations were made at the 1.23m telescope on Calar Alto Observatory, equipped with the TEK CCD #6 (1024×1024 pixels, FOV 8.5×8.5 arcmin). Between Jan and Mar 1996, observations were made at the 70cm telescope of Landessternwarte Heidelberg-Königstuhl (Germany), using a CCD camera with the GEC P8603 CCD (576×384 pixels, FOV 8×5.3 arcmin). Finally, observations with the 91cm Dutch telescope at ESO were made during a run from 1 to 11 May 1996. The instrument was a CCD camera with the ESO #33 TEK CCD (512×512 pixels, FOV 3.8×3.8 arcmin). During this run P1724 was observed once per night, at the beginning of the night. No standard stars were observed during these runs, and the photometry is therefore strictly differential. Instrumental magnitudes were obtained using PSF fitting routines from the IRAF[2] package `daophot`. We combined the data obtained at these three sites into our *RW* data set, and searched for periodicities as above. The same 5.7-day period is found (see Fig. 3e).

3. High-resolution spectra: the radial velocity

Our high-resolution spectroscopic observations of P1724 were obtained with the CfA echelle spectrographs, on the 1.5m Wyeth reflector (Oak Ridge Observatory, Massachusetts), the 1.5m Tillinghast reflector, and the 4.5m Multiple Mirror Telescope (both on Mt. Hopkins, Arizona). We collected a total of 40 spectra over a period of about one year and a half. For each exposure we used Reticon photon-counters to record a single echelle order (45Å) centered at 5187Å, with S/N ratios per resolution element ($8.5\ km\ s^{-1}$) ranging from 8 to 25.

Radial velocities were obtained by cross-correlation using the IRAF task `xcsao` (Kurtz et al. 1992), with a template selected from an extensive grid of synthetic spectra based on model atmospheres by Kurucz (1992a,b), calculated for us by J. Morse. These calculated spectra are available for a range of effective temperatures, projected rotational velocities, surface gravities and metal abundances (cf., Nordström et al. 1994, Latham et al. 1996). For our template parameters we adopted the values $T_{\rm eff} = 5000\ K$, $\log g = 3.0$, and $v \cdot \sin i = 70\ km\ s^{-1}$, which maximize the correlation, and we assumed solar metallicity. Small run-to-run velocity corrections were obtained from multiple exposures of the twilight sky, and applied systemat-

[2] IRAF is distributed by the National Optical Astronomy Observatories, which is operated by the Association of Universities for Research in Astronomy, Inc., under contract with the National Science Foundation.

Table 1. CfA radial velocity measurements for P1724.

HJD (2,400,000+)	RV ($km\ s^{-1}$)	HJD (2,400,000+)	RV ($km\ s^{-1}$)
49966.8419	+19.24	50145.6662	+25.38
49972.8691	+26.78	50149.6716	+21.58
49979.8857	+23.86	50151.6463	+26.05
50008.8803	+32.06	50357.9270	+19.65
50038.8219	+20.00	50360.0030	+30.84
50060.8449	+20.97	50379.8808	+23.45
50061.8424	+22.29	50385.8496	+18.77
50062.8643	+19.69	50389.8373	+21.06
50064.7093	+22.75	50406.9963	+29.72
50064.8558	+22.79	50407.9037	+22.73
50081.7864	+22.88	50408.8299	+12.57
50085.7732	+21.10	50411.8873	+26.35
50086.7738	+25.58	50438.8148	+23.58
50088.8303	+24.06	50448.7839	+14.31
50091.7655	+18.87	50472.6861	+24.92
50092.7866	+24.97	50473.7805	+25.94
50117.6842	+23.54	50474.7742	+27.76
50141.7177	+14.77	50494.6373	+17.42
50143.6424	+23.00	50495.7169	+26.71
50144.6548	+30.34	50497.6678	+28.86

Fig. 2a and b. (only in the electronic version of this paper) Radial velocity variation. **a** Power spectrum (with arbitrary power units) of the radial velocities showing a clear peak corresponding to a period of 5.7 days. **b** Radial velocity data phased with this 5.7-day period. This figure is available by ftp from CDS

ically to correct for instrumental shifts on all telescopes used (cf., Latham 1992). This effectively forces the same velocity zero-point on the three systems. Table 1 lists our RV measurements.

Although the resolution in $T_{\rm eff}$, $\log g$ and $v \cdot \sin i$ of our grid of synthetic spectra is designed for the purpose of velocity determinations, and small changes in the template parameters have little effect on the velocities, it is possible to invert the process to obtain estimates of the physical parameters of the star by interpolation, seeking to maximize the correlation averaged over all exposures. We have done this for P1724, and determined the following values for the effective temperature, surface gravity, and projected rotational velocity: $T_{\rm eff} = 4850 \pm 100\ K$, $\log g = 3.1 \pm 0.2$, and $v \cdot \sin i = 71 \pm 2\ km\ s^{-1}$.

A power spectrum analysis of our radial velocities clearly indicates the presence of a variation with a main period close to 5.7 days (Fig. 2). In the absence of concomitant photometric variations, one could argue that these velocity changes might be induced by a low-mass companion orbiting P1724, with a minimum mass of $0.087\ M_{\odot}$ (assuming that the primary has a mass of $3\ M_{\odot}$, see Sect. 5). However, brightness fluctuations with precisely the same period strongly suggest that rotational modulation by surface inhomogeneities (spots) is the likely cause (see also Sect. 6).

A sine curve fit through our radial velocity data gives a semi-amplitude of about $4.5\ km\ s^{-1}$ ($9\ km\ s^{-1}$ peak-to-peak), quite a significant effect (by virtue of the rapid rotation), implying also a fairly large spot coverage and/or large temperature differences with the surrounding photosphere. The addition of higher harmonics improves the fit only slightly, and the rms scatter remains at about $2.8\ km\ s^{-1}$. This is considerably larger than expected from similar material for a single star with similar exposure levels ($\sigma_{\rm RV} \sim 1.8\ km\ s^{-1}$; Nordström et al. 1994), even with a rotational broadening as large as that of P1724. It is likely that part of this excess scatter has to do with changes in the size, shape, temperature, location, or number of the surface features over the span of our observations, which would destroy the strict phase coherence otherwise expected from rotational modulation. Such changes are not at all unexpected in spotted stars.

Given the nature of the velocity variations and the scatter of the observations, our best estimate of the period from a simple sine curve fit to the spectroscopic data is 5.679 ± 0.004 days, nearly identical to the estimate in the previous section. The mean radial velocity from the same fit is $+22.3 \pm 0.5\ km\ s^{-1}$, although this is not necessarily the same as the center-of-mass velocity of the star (see next section).

Residuals from the fit show no evidence for further periodicities, from which we conclude that there are no spectroscopic companions to P1724 with orbital periods up to the duration of these observations, i.e. up to ~ 500 days, corresponding to a semi-major axis of $\sim 1.78\ AU$, or ~ 0.004 arc sec at $460\ pc$.

4. Long-term photometric variations

There is a considerable body of photometric observations for P1724 that goes back nearly 30 years. We have collected the absolute photometry in Table 2, where we also list the observations by Warren & Hesser (1977) and Cutispoto et al. (1996), in addition to our own CTIO observations in the $BVRI$ bands (Sect. 2) converted to the standard system, for use in the following section. The individual measurements by Cutispoto et al. (1996) have not been published previously, and were kindly provided by G. Cutispoto (priv. comm.). The 5.7-day periodicity in P1724 is evident in each separate data set over the entire span of the available observations, although strict coherence is probably not maintained. Indications of this from the radial velocity observations were already described above. Nevertheless, the spectroscopic data suggest that the spot characteristics are more or less stable for at least ~ 100 rotation periods (1.5 years), which is the duration of those observations.

The situation over longer time scales is illustrated in Fig. 3. In addition to the absolute photometry in the visual band from Warren & Hesser (1977) and Cutispoto et al. (1996), we show all the differential photometry in the same band (MTSB, CTIO, and *RW*; Sect. 2). Based on the discussions in previous sections, the period we have adopted for this comparison is $P = 5.679$ days. We fold and plot all the data throughout the remainder of the paper with the same period and epoch. The origin adopted for the phases is the date of the first of our Doppler imaging observations (see Sect. 6). The five light curves appear to be roughly in phase, although the uncertainty in the period is such

Table 2. UBVRIJHKL absolute photometric observations of P1724

Reference	JD$-2.4 \cdot 10^6$	U	B	V	R	I	J	H	K	L
Walker 1969	36488	12.86	11.96	10.65						
	37679	12.87	11.99	10.70						
	39111	12.77	11.90	10.64						
Warren & Hesser 1977	40144	12.66	11.71	10.45						
	40145	13.03	11.91	10.62						
	40178	12.66	11.77	10.50						
	40179	12.85	11.93	10.65						
	40183	12.67	11.77	10.52						
	40192	12.81	11.88	10.60						
	40193	12.73	11.81	10.54						
	40194	12.66	11.76	10.50						
	40195	12.69	11.78	10.52						
	40196	12.89	11.94	10.68						
	40197	12.97	12.00	10.71						
Penston et al. 1975	41635	12.54	11.72	10.44	9.44	8.71				
	42000							7.46	7.17	6.81
Breger et al. 1981	~ 42736								7.33	7.12
Cutispoto et al. 1996	48335.5301	12.86	11.58	10.70	9.97	9.23				
	48337.5156	12.75	11.49	10.60	9.86	9.15				
	48337.5255	12.68	11.41	10.55	9.83	9.10				
	48338.5306	12.84	11.55	10.66	9.93	9.20				
	48340.5194	12.89	11.59	10.74	10.01	9.26				
	48341.5392	12.82	11.53	10.68	9.95	9.20				
	48342.5180	12.71	11.43	10.56	9.83	9.12				
	48343.5212	12.70	11.43	10.56	9.83	9.11				
	48344.5255	12.88	11.58	10.69	9.95	9.22				
	48345.5159	12.91	11.62	10.75	10.02	9.28				
	48347.5192	12.78	11.50	10.62	9.90	9.16				
Preibisch et al. 1995	48976.901	13.11	12.11	10.72	9.94	9.24				
This work	50500						8.18	7.56	7.35	
	50112.6786		12.33	10.99	10.18	9.44				
	50112.7647		12.24	10.91	9.94	9.23				
	50113.5441		12.06	10.74	9.97	9.24				
	50113.6857		11.99	10.70	9.93	9.22				
	50114.5360		11.85	10.58	9.83	9.12				
	50114.6328		11.93	10.64	9.88	9.20				
	50114.7115		11.92	10.63	9.90	9.21				
	50115.6200		12.00	10.70	9.93	9.20				
	50115.6909		12.00	10.71	9.94	9.25				
	50116.6422		12.14	10.85	10.06	9.33				
	50116.7356		12.16	10.86	10.07	9.37				
(from all data)	brigthest	12.54	11.41	10.44	9.44	8.71	8.18	7.46	7.17	6.81
	faintest	13.11	12.33	10.99	10.18	9.44	8.18	7.56	7.35	7.12
	average	12.82	11.87	10.72	9.81	9.08	8.18	7.51	7.26	6.97
	stand. dev.	0.14	0.25	0.13	0.17	0.16	–	0.05	0.09	0.16

that the relative phasing over such long intervals is difficult to establish precisely. For example, a difference of only 0.0005 days in P leads to a phase shift of $\Delta\phi \sim 0.15$ between the Warren & Hesser (1977) data (epoch ~ 1968.8) and the more recent photometry, which we cannot rule out. Nevertheless, considering the long interval represented in fig. 3 ($\sim$30 years), the phase coherence displayed is quite remarkable.

Fig. 4 shows a sample of the color information available for P1724, folded in the same way as Fig. 3. From Figs. 3 and 4, we see that the color of the star is bluer when it is brighter, consistent with rotational modulation due to spots.

The relative phasing between the radial velocities (shown in the bottom panel of Fig. 3) and the recent photometry, which cover essentially the same time interval, is entirely consistent with this picture, as we show in more detail in Sect. 6. The minima/maxima in the RV curve (Fig. 3f) are shifted by ~ 0.25 in phase compared to the photometry (Fig. 3a-e). This is exactly what one expects from a spot on the star: The max/min RV

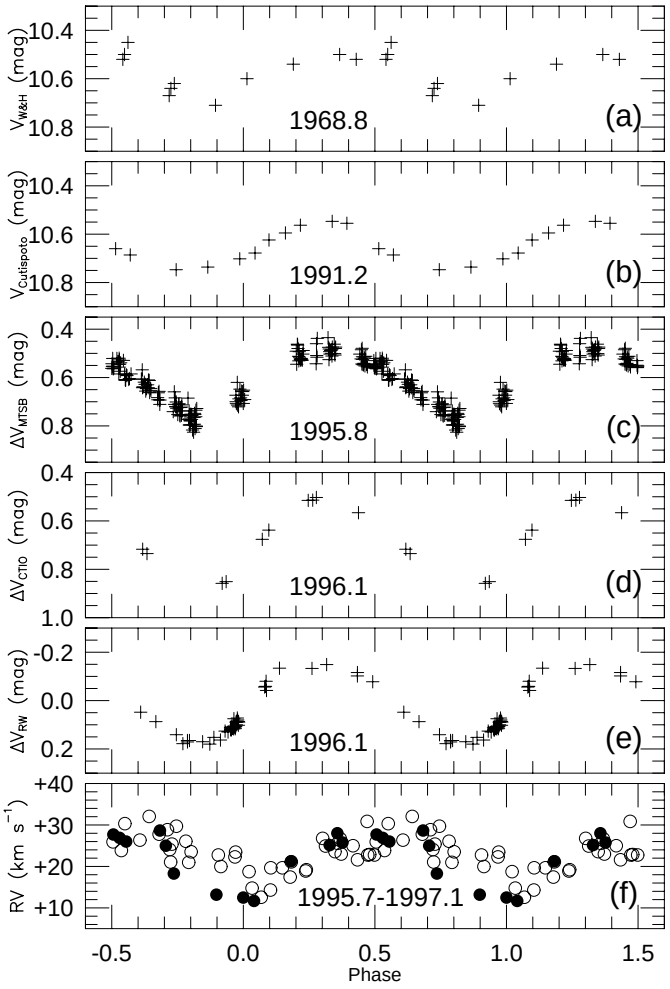

Fig. 3a–f. The 5.7-day periodicity in the brightness and the radial velocity of P1724 over 30 years. We show all the available photometry in the V band that covers a significant fraction of the cycle: **a** Warren & Hesser (1977); **b** Cutispoto et al. (1996); **c** MTSB; **d** CTIO; **e** *RW*. Also shown in **f** are the radial velocities (RV) from CfA (open circles) and from our Doppler imaging observations (filled circles). All observations have been folded with the same period $P = 5.679$ days, and the vertical scale on the top five panels is the same to facilitate the comparison; the same origin is adopted here as in the Doppler imaging analysis below, namely, JD 2450067.70257; the mean epoch of the observations is shown in each data set

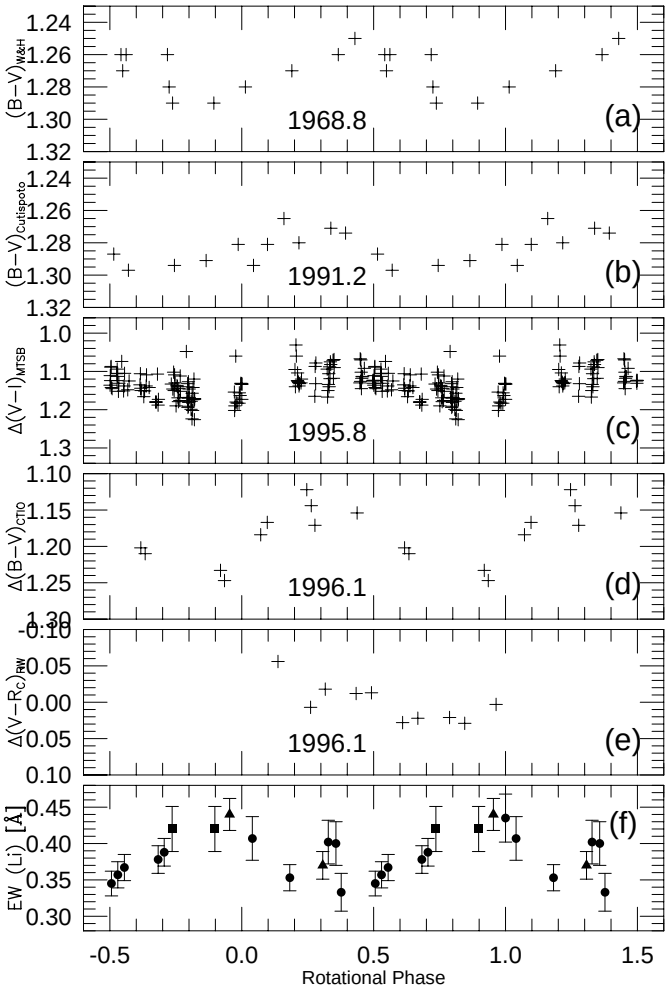

Fig. 4a–f. Rotational modulation in the color indices. We show, from top to bottom, **a** $B-V$ from Warren & Hesser (1977), **b** $B-V$ from Cutispoto et al. (1996), **c** $\Delta(V-I)$ from our MTSB data, **d** $\Delta(B-V)$ from our CTIO data, **e** $\Delta(V-R_{\rm C})$ from *RW*, and **f** equivalent width of the lithium 6708Å line (see Sect. 7 for details); ephemeris as in the previous figure

occurs not when the spot is crossing the center of the disk (when the photometry is at a minimum), but rather when the spot is between the disk center and the limb.

Because the Doppler shifts we measure are actually produced by the presence of surface features, it is difficult to determine the velocity of the center of mass of the star accurately. In principle the most representative values are those when the spot(s) are distributed symmetrically on the disk, either in front or behind, which corresponds to minimum or maximum brightness, respectively. Under this assumption we estimate from the curves in Fig. 3 a mean value $RV = +23 \pm 1\ km\ s^{-1}$.

The photometric observations for P1724 show some evidence for changes in the brightness at maximum light. Fig. 5 displays all the available data in the V band that are on the standard system. The dotted line drawn through the highest points suggests a dimming of roughly 0.15 mag over the past $\sim$ 30 years. In addition, the amplitude of the variation in the V band seems to have increased, as determined from sine curve fits to the data from Warren & Hesser (1977) (~ 1968.8), Cutispoto et al. (1996) (~ 1991.2), MTSB (~ 1995.8), CTIO (~ 1996.1), and *RW* (~ 1996.1). From our sine curve fits, we obtain ΔV of 0.20, 0.20, 0.27, 0.36 and 0.34 mag, respectively, for the data sets listed above, with uncertainties ~ 0.01 to 0.02 mag. Both of these changes – overall dimming and growing amplitude – are consistent with a gradual increase in the spot coverage and/or a decrease in spot temperature over time.

Our CfA radial velocity monitoring covered ~ 1.5 years, i.e. many rotation periods. As discussed above, we do see some indication of changes in the spot(s) in those data. However, it is difficult to investigate the details of any phase drifts over such

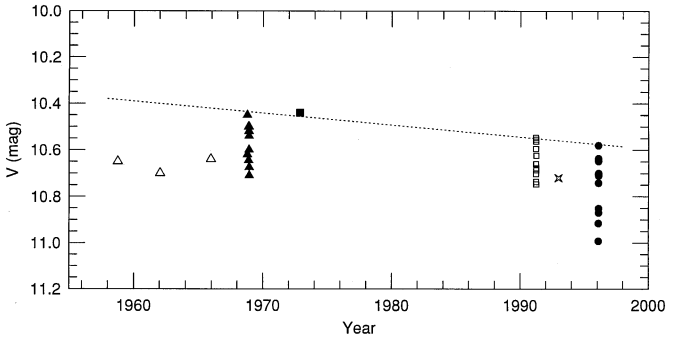

Fig. 5. Long-term variations in the V band. The figure shows all available observations in the standard system, as a function of date. The dotted line drawn through the highest points suggests a gradual decrease in brightness

a long period ($\sim$ 30 years) from photometric data sets that are rather sparse and inhomogeneous. We can only conclude here that the spot(s) seems remarkably stable, but we cannot rule out small phase shifts with the data available.

If the photometric and RV variability are indeed due to spot(s), then one would perhaps expect to see a much faster evolution in phase of the variable quantities, as suggested by the solar analogy, mainly due to spot migration. We point out, however, that P1724 is a very young object quite different from the Sun, and one should therefore not necessarily expect rapid spot evolution as in older stars. In fact, in the case of the wTTS V410 Tau, the spot distribution is dominated by a large decentered polar spot that appears to be very long-lived – certainly lasting several years, and possibly more than a decade (Hatzes 1995). There are many other documented cases of long-lived spots lasting a decade, and even longer with very little change in the apparent rotational period (e.g., Hall & Busby 1990, Oláh et al. 1997).

5. The spectral energy distribution of P1724, and its location in the H-R diagram

In order to investigate the spectral energy distribution (SED) of P1724 and derive its bolometric luminosity, we have made use of all available $UBVRIJHKL$ photometry from the literature (Walker 1969, Penston et al. 1975, Warren & Hesser 1977, Breger et al. 1981, Preibisch et al. 1995, and Cutispoto et al. 1996). Our own $BVRI$ observations obtained at CTIO are also useful (Table 2), but the MTSB and *RW* measurements cannot be reliably placed on the standard system. In addition, we obtained new data at JHK to supplement the previous observations.

Our new observations in the JHK bands were obtained on 20 Feb 1997 at the CTIO 1.5m using the CIRIM array, and are listed also in Table 2. They were obtained in a 3×2 raster pattern, with 15 arc sec offsets. Three frames were exposed and co-added at each raster position. The total integration time on P1724 was 7.2 seconds through each of the K, H, and J filters. The data were flat-fielded using dome-flats, co-added, median-filtered, sky-subtracted, then co-aligned and summed. Five or six standard stars (Elias 1981) were observed nightly. Uncer-

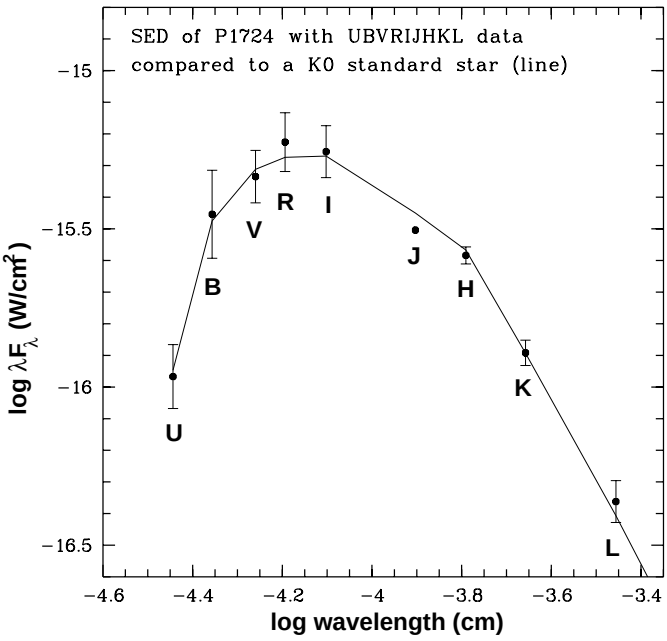

Fig. 6. Spectral energy distribution of P7124. The SED for P1724 from UBVRIJHKL photometry with the average data and the standard deviations as listed in Table 2, compared to a K0 standard star. P1724 is neither detected in M (Breger et al. 1981, $M > 5.65$ mag) nor by IRAS (Weaver & Jones 1992)

tainties in the magnitudes, based on the scatter in the standard star solutions, are ± 0.02 mag. All CIRIM data reductions were performed using IDL.

Because the observations collected in Table 2 are not simultaneous, they are significantly affected by the photometric variations in P1724 due to rotational modulation by spots, which is much larger than the precision of these measurements. In addition, there are probably also long-term variations as discussed in the previous section. Further evidence of these changes is given by the range of spectral types reported for the star over the years: G8 (Herbig & Bell 1988 and Tagliaferri et al. 1994), K0 (Van Altena et al. 1988), K2 (Terranegra et al. 1994), and K3 (Preibisch et al. 1995). Variations in the spectral type of this order are typical for spotted stars (e.g., Bouvier et al. 1993).

As a compromise, we have adopted the average between the maximum and minimum values in each band for the determination of the SED and the calculation of the bolometric luminosity. This SED is thus an *average* one. We compared the observed SED of P1724 with those of standard stars with spectral types in the range from mid-G to mid-K. We find the best match for a spectral type of K0 (see Fig. 6).

The SED in Fig. 6, corrected for extinction, shows that P1724 has neither significant UV nor significant infrared (IR) emission in excess of the standard star. Hence, we may classify it as a naked TTS. Because the $H\alpha$ equivalent width (0.7 to 2Å; cf. Sect. 7) and flux are very weak, it may also be considered a wTTS. [3]

[3] While wTTS, by definition, show weak $H\alpha$ emission measured usually as equivalent width, naked TTS lack any IR excess emission

The extinction and bolometric luminosity were estimated as described in detail by Alcalá et al. (1997). We obtain $L_{bol} \simeq 49\ L_{\odot}$, an extinction of $A_V \simeq 1.6$ mag [4], and from these a radius of $\simeq 9.1\ R_{\odot}$ derived from the Stefan-Boltzmann law. If we use instead the Barnes-Evans relation (Barnes & Evans 1976), we obtain a radius of $\simeq 8.9\ R_{\odot}$, again adopting $460\ pc$ as the distance. The IR photometry is intrinsically less precise than the optical data, but at the same time less sensitive to the effect of spots. We repeated the luminosity and radius calculations using the optical and IR bands separately, and obtained internally consistent results as when using all the photometry together. This indicates that the results are quite robust. For the remainder of the paper we adopt $9\ R_{\odot}$ for the radius.

By comparing the locus of P1724 in the H-R diagram with theoretical tracks and isochrones, we can estimate its age and mass. From both the Forestini (1994) and the D'Antona & Mazzitelli (1994) models, we derive an age of $\sim 2 \times 10^5$ years and a mass [5] of $\sim 3\ M_{\odot}$. P1724 appears to be slightly more massive in the Palla & Stahler (1993) model for intermediate-mass Herbig Ae/Be stars. Hence, as far as the mass is concerned, P1724 appears to be a star near the borderline between TTS and Herbig Ae/Be stars. P1724 is clearly a pre-MS star; post-MS stars with spectral type G0 or later show much weaker lithium than P1724 and/or rotate slower than $v \cdot \sin i = 10\ km/s$ (Gray 1989).

The mass and radius of P1724 from the SED yield a surface gravity ($\log g \approx 3.0$) in excellent agreement with our spectroscopic gravity determination ($\log g = 3.1 \pm 0.2$, Sect. 3). The surface gravity obtained from Strömgren photometry by Terranegra et al. (1994) yields $\log g = 3.7 \pm 0.5$ according to Tagliaferri et al. (1994), also consistent with our results within the errors. However, activity in general is known to affect Strömgren photometry (Morale et al. 1996, Alcalá et al. 1998). Our high-resolution spectroscopy yields a gravity independent of the distance (Sect. 3), which is consistent with the above distance-dependent measurements. This can be taken as an additional indication that P1724 is most likely located at the distance of the Orion nebula.

6. High-resolution spectra: Doppler imaging

Additional high-resolution observations collected primarily at McDonald Observatory comprise a timeseries over the rotational period of P1724. The photospheric absorption lines clearly show the types of distortions common to heavily spotted late-type stars, though the line wings tend to vary more than is usually seen. Since there is no compelling evidence in spectroscopic or photometric data sets of a companion which could cause such oscillations, we proceed under the assumption that the distortions are indeed a product of surface temperature inhomogeneities. We can also assume that P1724, as a TTS, does not rotate differentially (Johns-Krull 1996). Image reconstructions are presented herein.

Table 3. P1724 Doppler Imaging observing log. We list for each high-resolution observation the heliocentric Julian date, the rotational phase counted from the middle of the first of our exposures, the heliocentric radial velocity in km/s (typically ± 2 to $3\ km/s$), the equivalent widths for the Li 6708Å, Fe 6430Å, Ca 6439 and the $H\alpha$ emission lines, as well as the (log of the) $H\alpha$ flux (in $erg/s/cm^2$). The last two spectra were obtained with CASPEC at the ESO 3.6m and the others with the McDonald 2.1m telescope.

$HJD-$	Φ_{rot}	RV	equivalent width in mÅ				log
2450067			Li	Fe	Ca	$H\alpha$	$F_{H\alpha}$
0.70257	0.000	12	435	271	364	-1805	6.87
0.93246	0.040	12	407	334	279	-1648	6.81
1.73385	0.182	21	353	281	282	-2615	7.06
19.60582	3.328	25	402	283	340	-2023	6.96
19.76858	3.357	28	400	245	324	-1996	6.95
19.87923	3.377	26	333	232	303	-2155	6.97
20.61548	3.506	28	345	317	294	-2572	7.04
20.74903	3.530	27	357	282	303	-2615	7.04
20.89112	3.555	26	367	264	299	-2023	6.93
21.61889	3.683	29	378	238	300	-1962	6.87
21.74922	3.706	25	388	235	313	-2176	6.88
44.63733	7.723	18	440	272	296	-2667	6.99
45.55653	7.898	13	420	267	301	-1817	6.84

6.1. Data acquisition and reduction

High resolution spectral observations were made using the Sandiford Cassegrain Echelle spectrograph at McDonald Observatory's 2.1m telescope. This instrument is a prism cross-dispersed echelle used with a Reticon Corporation 1200×400 pixel CCD. This combination provides a wavelength coverage of up to 1500Å at a resolving power as high as 60000 (McCarthy et al. 1993). The instrumental setup for the P1724 observations yields a wavelength coverage from 6000 to 7500Å with a resolution of 0.18Å (3 pixel slit) at 6400Å, corresponding to $R = 38000$.

The data were reduced using the IRAF `echelle` package, which consisted of the standard bias subtraction, global scattered light subtraction, division by a properly calibrated flat-field frame, and order extraction. To complement this data set and provide us with more complete phase coverage, we also used the high resolution CASPEC spectra described below in Sect. 7. Table 3 summarizes the observations used in the Doppler imaging (DI).

Radial velocities for each individual observation are determined using a cross-correlation method similar to that out-

(Walter 1986). All naked TTS also are wTTS, but some wTTS are not naked. E.g., SU Aur shows low $W_{\lambda}(H\alpha)$ (Cohen & Kuhi 1979, Cabrit et al. 1990), yet has a very luminous disk (Strom et al. 1989, Beckwith et al. 1990).

[4] This is quite large for a naked wTTS, but see Sect. 9. Preibisch et al. (1995) gave a smaller value, namely $A_V \simeq 1$ mag, which was determined from their photometry taken when P1724 was particularly faint, i.e. when the spot was in front, so that not only the extinction appeared to be smaller, but also the spectral type they gave, as determined from the spectrum, was slightly later (K3), because of the contribution of the spot.

[5] For this estimate, we have extrapolated slightly beyond the highest mass track available, which is $2.5\ M_{\odot}$.

Fig. 7. (only in the electronic version of this paper) Doppler imaging line fits. The observed absorption lines (open circles) in the timeseries are plotted with the model fits (solid lines) for each of the five lines used in this analysis. Also plotted are the residual vectors (in the sense: $data - model$) to illustrate that no systematic features appear above the noise level that the code may have failed to fit. The average of all residuals is plotted along the bottom. This figure is available by ftp from CDS

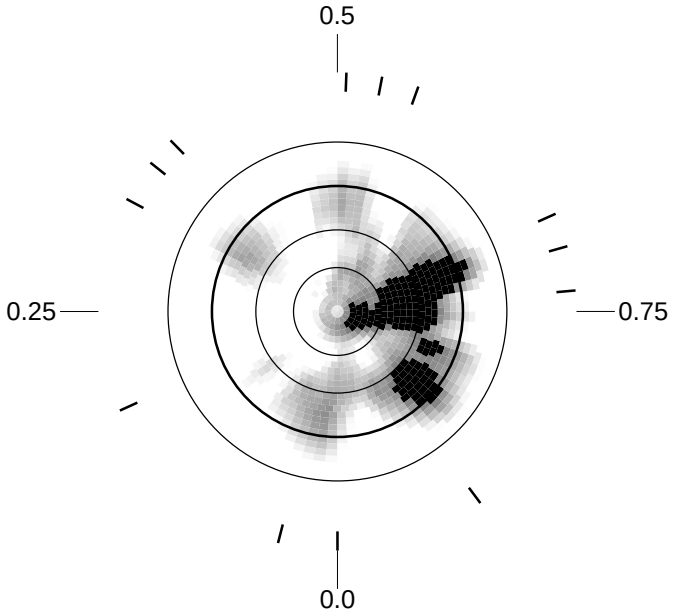

Fig. 8. Doppler image. The Doppler image reconstruction of P1724 as a polar projection down to a latitude of 30° S latitude. The image shown is the average of the images from each timeseries. Tick marks around the periphery note the rotational phases at which the star was observed. The thick line marks the stellar equator

lined in Tonry & Davis (1979). Since P1724 has been classified as late G to early K, we use the NSO full disk solar spectrum (Kurucz et al. 1984) as the non-rotating template in the cross-correlation. The peaks of Gaussian fits to the cross-correlation functions define the radial velocities. The spectral regions between $6080-6150$Å, $6130-6190$Å, $6180-6240$Å, $6380-6450$Å, and $6440-6510$Å contain clearly defined absorption lines and few telluric features which is what the method requires. We therefore rely on these wavelength regions in computing the cross-correlation functions.

It is expected that distortions in line profiles due to surface temperature inhomogeneities will skew the Gaussian peaks, and we measure the resulting dispersion. From our rotational timeseries, we compute a mean radial velocity of $+23.5\ km\ s^{-1}$ and a standard deviation of $6.4\ km\ s^{-1}$. This is consistent with the results from the low S/N high-resolution spectroscopy presented in Sect. 3.

6.2. Doppler image reconstruction

The algorithm described by Vogt et al. (1987) is used to reconstruct images of the stellar surface. The method uses a maximum entropy regularization to constrain the solution. It does not simultaneously consider broad-band continuum light curves, but we use this information in determining the final spot temperatures.

Doppler image reconstruction uses a rotational timeseries of absorption line profiles to ascertain spatial information. It requires that absorption lines are not significantly blended within the wavelength interval defined by the rotational velocity. The spectral format is scoured for such lines using the solar spectrum for reference. Some lines, though ideal, are rejected because of contamination from telluric lines. We choose the absorption lines Fe I $\lambda 6393.6$Å, Fe I $\lambda 6430.8$Å, Ca I $\lambda 6439.1$Å, Ti I $\lambda 6643.6$Å, and Ti I $\lambda 7122.2$Å for the analysis, each defining a separate timeseries.

The method also requires knowledge of the specific intensity profiles as a function of limb angle across the stellar disk. These are obtained using the spectral synthesis package, SME (Valenti & Piskunov 1996), atomic line data from the Vienna Atomic Line Database (VALD, Piskunov et al. 1995), and the grid of Kurucz model atmospheres (Kurucz 1993). SME computes LTE models and uses a non-linear least squares algorithm to solve for any indicated free parameters. For our program star, we assume solar metallicity and a surface gravity of $\log\ g = 3$ (as determined in Sect. 3). We let SME solve for $T_{\rm eff}$, microturbulence, and $v \cdot \sin i$. Since there are undoubtedly errors in all parameters, we expect to obtain slightly different results for each line as the code tries to compensate for errors in the fixed parameters, atomic data, and atmospheric models. This is acceptable since we are primarily concerned with constructing a well-matching fit to the disk integrated line profile (Stout-Batalha 1997). The solution is determined by matching the model to the average of all profiles in the timeseries. SME gives us $T_{\rm eff} \simeq 5000\ K$, a mean microturbulence of $2.3\ km\ s^{-1}$, and $v \cdot \sin i \simeq 75.5\ km\ s^{-1}$, all consistent with the results in Sect. 3.

The inclination angle is computed assuming a rotational period of 5.679 days, a radius of $9\ R_\odot$ (cf. Sect. 5), and $v \cdot \sin i \simeq 71\ km\ s^{-1}$, which is our best estimate of the rotational velocity (cf. Sect. 5). This gives an inclination angle of $i = 62^\circ$.

6.3. Doppler imaging results

Our line fits for the Doppler imaging are presented in Fig. 7a,b. The final Doppler image of P1724 is shown in Fig. 8 as a polar projection down to a latitude of -30°. The assumed inclination of the star's rotational axis, $\sim 62^\circ$, does not allow us to see below this latitude. The image is actually the average of the five individual images reconstructed from each of the five timeseries (one for each spectral line selected). While we do not display all images here, we note their high degree of correlation as quantified by the linear Pearson correlation coefficients listed in Table 4. Individual image reconstructions and a more thorough comparative analysis can be found in Stout-Batalha (1997).

As expected, we find evidence of low to intermediate latitude surface features as demanded by the large velocity excursions of the absorption line wings. More specifically, we find

Table 4. P1724 Doppler imaging linear correlation coefficients.

	Fe I λ 6393.6	Fe I λ 6430.8	Ca I λ 6439.1	Ni I λ 6643.6	N II λ 7122.2
Fe I λ 6393.6	1.000	0.667	0.684	0.706	0.677
Fe I λ 6430.8	–	1.000	0.718	0.802	0.776
Ca I λ 6439.1	–	–	1.000	0.767	0.764
Ni I λ 6643.6	–	–	–	1.000	0.774
N II λ 7122.2	–	–	–	–	1.000

a predominant spot (or spot group [6]) near phase 0.75 and centered at a latitude of approximately $+30°$. This feature is easily seen as a distortion near the line center of the absorption lines taken at phase 0.71. There is also evidence of lower level features between 0 and $+30°$ which persist upon image averaging. However, most of these features are located at sub-observer longitudes and are therefore likely artifacts of the algorithm, an artifact referred to as *phase-ghosting* which is discussed in more detail in Stout-Batalha (1997). The size of the spotted area is $\sim 12\ \%$ of the visible disk.

The average temperature of the predominant spot group is obtained by comparing the V-band photometric observations with the artificial light curve which our image reconstruction produces. We find that a local temperature $800\ K$ cooler than the surrounding photosphere (taken to be $5000\ K$) reproduces the observed light curve amplitude best. This is only a $100\ K$ decrease relative to the minimum temperature found in the average image reconstruction. The total spot area assigned this temperature is represented in Fig. 8 by the black-shaded region.

From the temperature of the spot and the physical parameters of the surrounding photosphere, we can estimate the strength of the magnetic field assuming equipartition and the ideal gas equation. With $3\ M_{\odot}$ and $9\ R_{\odot}$ as obtained above for P1724, along with a value of $\mu = 0.6$ for the mean molecular weight, we obtain a gas pressure of $\sim 142900\ g/cm/sec^2$ which then corresponds to a magnetic field of $\sim 1.9\ kG$ for P1724. This is quite similar to those measured in other TTS (Basri et al. 1992, Guenther & Emerson 1996) though perhaps somewhat larger.

Fig. 9a shows the modeled versus the observed light curve. The photometric observations that are closer in time to the Doppler imaging observations (the *RW* data set) have been phased relative to the HJD at mid-exposure of our first high-resolution observation. In generating the model RV curve, the re-constructed spot distribution was first converted into a two temperature distribution. All image pixels more than $500\ K$ cooler than the photospheric temperature were assigned a temperature $800\ K$ cooler than the photospheric value; all image pixels less than $500\ K$ cooler than the photospheric temperature were replaced by the photospheric value. This was done primarily because the re-construction process produces a smooth temperature variation from spot to photosphere, even if the real distribution is a discrete distribution. Furthermore, the maximum entropy method tends to make spots warmer than they actually are. Finally, a two temperature distribution is more consistent with the solar analog. The agreement between the predicted and observed light curve is excellent.

Shown in Fig. 9b are the measured radial velocities plotted as a function of rotational phase, together with those predicted by the same 'thresholded' image used in generating the predicted light curve. This image was used to generate a set of synthetic Fe I 6430Å and Ca I 6439Å profiles with good phase coverage that were then used for computing the radial velocity. Again, there is good qualitative agreement in the shape of the variation, although the predicted amplitude is less than the observed one.

The reader is cautioned, however, that the predicted RV curve should be regarded more as a qualitative one for the following reason: The DI algorithm cannot predict with great accuracy the amplitude of the distortions in the absorption lines. This amplitude depends on exactly what the line profile and continuum look like in the spotted regions, which we do not know with certainty. The DI algorithm makes the simplifying assumption that the equivalent width of the line is the same in the spot and photosphere. It determines the continuum value in the spot simply by scaling the photospheric continuum flux (at the appropriate limb angle) by a black-body relation to reflect the spot temperature. These two assumptions work to under-estimate the amplitude of the distortion in the line profile. The smaller distortions manifest themselves in the predicted RV curve by decreasing the amplitude of the variations. We see exactly that in Fig. 9b. However, the shape of the predicted curve is in very good agreement with the observations.

For the sake of argument we mention here that it is still possible that there is a close, possibly even sub-stellar, spectroscopic companion which produces part of the radial velocity variations. We have tested this possibility by subtracting the DI model prediction on the RV variability (specifically for the Fe line as plotted above in Fig. 9b) from our actual RV data to obtain a residual variability. We then searched for periodic signals in these residual velocities, and found a 6.5 day period. Assuming for the moment that this excess variation is caused by a companion, an orbital fit through these residuals gives a semi-amplitude of $\sim 5\ km/s$ and a high eccentricity of 0.64. The corresponding minimum mass of such a companion would be $\sim 70\ M_{jup}$. [7] However, the rms scatter around this orbit

[6] From our observations, we cannot distinguish whether the surface feature is made up of one or several spots. Donati et al. (1997) recently found evidence that the dark surface feature on V410 Tau is composed of one dark spot, from a strong signal measured by performing spectropolarimetry.

[7] From this estimate ($M \cdot \sin i = 70\ M_{jup}$) and the assumption that this object, if it exists, orbits in the equatorial plane of P1724 (known to be inclined to the line-of-sight by $i = 62°$, see above), we obtain

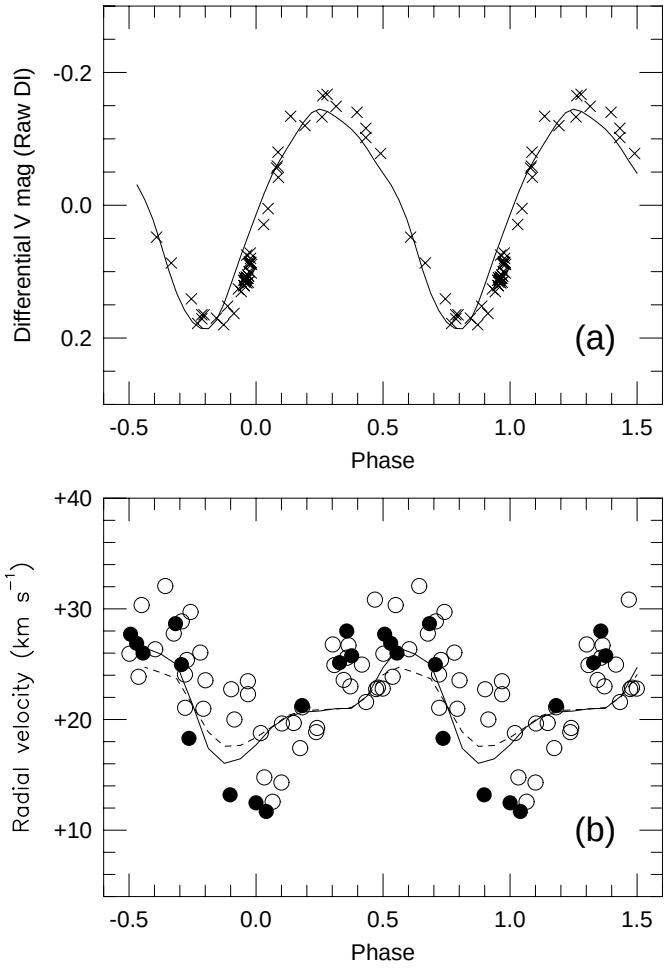

Fig. 9a and b. Observed V band and radial velocity variations compared to the DI model predictions. The differential photometry by *RW* is shown in the top panel, and in the lower panel we include the CfA velocities (open circles) and those from the spectra used for the Doppler imaging reconstruction (filled circles) listed in Table 3. The full line is for the synthetic Fe I 6430Å line only, and the broken line for Ca I 6439Å

is fairly large, about $2.9\ km/s$. Since this is about the same as the scatter from a Keplerian orbit fit to the raw CfA velocities ($2.8\ km/s$ as given above), we do not find the companion hypothesis very compelling. The uncertainties in the DI model prediction of the RV curve are probably large enough to explain the difference with the observational data without the need for additional components. Our analyses suggest that spottedness is most likely the sole cause of the variability. If there is a close companion to P1724, we do not find conclusive evidence for it in our data.

The low latitude ($+30°$) of the predominant spot group on this object stands in contrast to those found in other image reconstructions of TTS. HD 283572 (Joncour et al. 1994b), V410 Tau (Joncour et al. 1994a, Strassmeier et al. 1994, Hatzes 1995, Rice & Strassmeier 1996), and Sz 68 (Johns-Krull & Hatzes 1997) all show evidence of high latitude features (above $+60°$). One parameter separating these objects from P1724 is the rotational period. All three previously analyzed TTS have rotational periods ≤ 2 days while P1724 rotates with a period of 5.7 days. The theoretical models of Schüssler et al. (1996) predict that magnetic flux tubes will emerge at higher latitudes on the stellar surface for higher rotation rates. They also predict that the emergence latitude depends strongly on the depth of the convection zone in that a deeper convection zone leads to higher latitude emergence. Among the TTS imaged, P1724 is the most massive with $\sim 3\ M_{\odot}$ (see Sect. 5). Though placement in the HR diagram (see Sect. 5) puts it close to the stellar birth line, stars of this mass quickly develop a radiative core thereby reducing the depth of the convection zone. These factors may contribute in producing the low latitude surface features.

Even if the phasing appears to be stable for ~ 30 years, it is still possible that some small differential rotation and spot migration are present, but counteracting; we believe, though, that this is rather unlikely. The dominant spot we see on P1724 may also be indicative of a global (oblique) dipole field. As mentioned earlier, there have been a number of reports regarding spots on late-type stars lasting for a decade or even longer (e.g., Hall & Busby 1990, Oláh et al. 1997), so that P1724 does not appear to be such an extreme case.

We conclude that the modulations in the high resolution absorption line spectra of P1724 are well explained by surface temperature inhomogeneities, the distribution of which is weighted at phase 0.75 and $30°$ latitude. These results have expanded the parameter space for theoretical work on rapidly rotating, spotted stars.

7. Optical spectra: Ca II, $H\alpha$, and lithium

In this section we investigate some youth and activity indicators for P1724, namely lithium absorption as well as Hα and Ca II H & K emission.

Two high-resolution spectra were obtained at the European Southern Observatory (ESO) on 29 and 30 Jan 1996 using the 3.6m telescope and CASPEC (Pasquini 1993 and references therein), covering the wavelength range from $\simeq$ 5700 Å to $\simeq$ 7950 Å. The 31.6 lines mm^{-1} echelle grating was used together with the red cross-disperser (158 lines mm^{-1}) and the long camera (focal length $=$ 560 mm, f/3). The above combination, together with ESO CCD #37 (TK1024AB, with 1124×1024 pixels^2 of 24 μm^2) and a slit aperture of 200 μm ($\sim 1.4''$ on the sky), resulted in a nominal resolving power of $R \sim 20000$. The slit height was set to $5''$, giving enough inter-order spacing to allow the subtraction of scattered light. Data reduction was performed using the echelle reduction package available within the Munich Image Data Analysis System (MIDAS, version Nov95), with the addition of some specially developed procedures making use of the algorithms prescribed by Verschueren & Hensberge (1990) for background subtraction and optimal order extraction. The reduction included tracing of the echelle orders, fitting and subtraction of the background

$\sim 79\ M_{jup}$ for the companion mass, i.e. very close to the hydrogen burning limit (being $\sim 80\ M_{Jup}$), so that this companion might even be a brown dwarf; see, e.g., Kulkarni 1997 for a recent review.

from all frames, fitting of the blaze function and normalization to the continuum, extraction of echelle orders, wavelength calibration using thorium calibration lamp exposures taken at the same telescope position of each individual science frame, and merging of the orders.

Additional high-resolution spectra were obtained on 22 and 24 Jan 1997 using the KPNO 4.0m echelle [8]. We used the long red camera and the T2KB CCD. Observations were taken through the $150\mu m$ ($\sim$1.2 arc sec) slit. The first spectrum was made through thin cirrus, with about 1.5 arc sec seeing; on 24 Jan, the seeing was sub-arc second. Both sets of observations consisted of three 500 sec integrations. The spectra cover the range 4275 to 7385Å in 54 orders, at a resolution of ~ 35000. We obtained projector flat images to flatten the spectra. A Th-Ar comparison source was observed before and after each telescope slew. Initial reductions were undertaken at KPNO, using the IRAF `doecslit` package. We corrected for bias, extracted the orders, divided by the flats, and solved for the dispersion. The data were rebinned to a linear wavelength scale in each order and further reduced using IDL. The spectra were flattened in each order to remove any residual curvature left from the original flat division. We trimmed 510 points from the ends of the orders, leaving 1534 points per order. We then filtered the three individual spectra of each night to remove cosmic rays and co-added the spectra. The resulting spectra have S/N in excess of 100 per pixel near 6700Å, but the S/N is considerably less towards the blue. No attempt was made to reduce the counts to flux.

In addition to these relatively high-resolution spectra, we obtained three low-resolution spectra on 21, 25, and 26 July 1996 at the European Southern Observatory (ESO) using the 1.52m telescope equipped with a Boller & Chivens spectrograph. A 900 grooves/mm (ESO # 5) grating and the CCD FORD $2048L$ of 2048×2048 pixels were used. With this set-up a mean resolution of ~ 2.5 Å (FWHM) in the 4400 to 7000 Å spectral range was achieved. The reduction of these spectra was carried out using the MIDAS package. Bias and dark subtraction was first performed on each frame. The 2-D frames were then divided by a mean flat-field and then calibrated in wavelength. Finally, sky subtraction was performed.

Another low-resolution spectrum was obtained with the Calar Alto Faint Object Spectrograph (CAFOS) at the 2.2m telescope of the Calar Alto Observatory, Spain, on 20 Dec 1996. We used the red grating G2, giving a mean resolution of ~ 3.5 Å (FWHM) in the spectral range of 3400 to 6300 Å. The reduction was carried out with the MIDAS package: bias and dark subtraction, dividing by a mean flat-field, wavelength calibration, and sky subtraction.

According to Soderblom et al. (1993), the presence of dark spots inhomogeneously distributed on the stellar surface can produce rotational modulation of the lithium 6708Å line strength since this line is quite temperature sensitive. Under extreme conditions, the abundance can appear to be larger by up to several tenths of a dex. We can check this with our data: The Li line should appear to be stronger when the spot is in front. For checking this, we use the W_λ(Li) values obtained with our high-resolution spectra at McDonald, ESO 3.6m CASPEC (see Table 3), and KPNO (W_λ(Li)$= 0.44$Å on 22 Jan 1997 and W_λ(Li)$= 0.37$Å on 24 Jan 1997). Since the Li strength may be overestimated in low-resolution spectra (Covino et al. 1997), we do not use our low-resolution spectra for this particular investigation.

The data are displayed in Fig. 4f, which clearly shows rotational modulation of W_λ(Li): It appears to be lowest near phase 0.4, i.e. when the star is brightest, i.e. when the spot is on the back side, as expected. Rotational modulation of W_λ(Li) has not been seen before, except very recently in the wTTS V410 Tau: Fernández & Miranda (1998) have studied their own spectroscopic monitoring data of V410 Tau obtained almost simultaneously with published photometric monitoring by Petrov et al. (1994). Fernández & Miranda found a peak-to-peak variability in V of 0.6 mag and a peak-to-peak variability in W_λ(Li) of 0.12Å clearly in phase with the well-known rotation period of V410 Tau. Neither such a large variation in W_λ(Li) nor its rotational modulation has been seen in V410 Tau before, although the star had been observed often. Whenever other authors (Patterer et al. 1993, Welty & Ramsey 1995) monitored this star in V or W_λ(Li), its variation in both V and W_λ(Li) were significantly lower – except Strassmeier et al. (1997), who found a variation in V of 0.65Å. Also, a number of Pleiades stars monitored by Soderblom et al. (1993) that do not exhibit any rotational modulation of W_λ(Li) show much lower variation in V, namely below 0.1 mag. Hence, the larger the V mag variation, the stronger the rotational modulation of W_λ(Li) is, which is consistent with our results on P1724, where we see a large V-band variation together with rotationally modulated Li 6708Å line strength.

Other absorption lines also appear to be variable, namely the Fe I 6431 and Ca I 6439 lines used in the DI analysis (see Table 3). However, these lines are slightly weaker than the Li I 6708 line making it more difficult to detect rotational modulation with confidence. Furthermore, these lines are not as temperature sensitive as the lithium line. We would thus expect a smaller amplitude variation. Rotational modulation is therefore difficult to quantify for these lines with the given S/N.

To obtain the proper lithium abundance, we must use the W_λ(Li) value near phase 0.4, when it is not affected by the spot. This gives W_λ(Li)$= 0.34$Å. From the NLTE curves of growth from Pavlenko & Magazzù (1996), and using the measured gravity, effective temperature, and the above lithium equivalent width, and considering the errors, we obtain the lithium abundance of $\log$N(Li)$= 3.25 \pm 0.10$, in the customary scale

Fig. 10a–h. (only in the electronic version of this paper) Red spectra of P1724. Low-resolution: **a**-**c** ESO 1.5m Boller & Chivens spectra, and **d** Calar Alto 2.2m CAFOS spectrum. High-resolution: (**e**,**f**) KPNO 4.0m echelle spectra, and (**g**,**h**) ESO 3.6m CASPEC spectra. We show flux versus wavelength, and we indicate the $H\alpha$ and lithium lines with dotted lines. This figure is available by ftp from CDS

[8] These two spectra could not be used for the Doppler imaging analysis, as they are separated by one year from the other observations.

where $\log\ N$(H)$= 12$. This is consistent with the primordial value, to be expected for this star with its very young age and its relatively high mass [9].

An additional timeseries of the $H\alpha$ chromospheric lines is shown in Fig. 11, from the observations listed in Table 3. In Figs. 10 and 11, we see a wide variety of profile characteristics: broad and narrow emission line components, asymmetries, double-peaked profiles, multiple absorption components, and variable flux. We seek to determine whether this variability is rotationally modulated and if so, whether it is correlated with the photospheric active regions mapped above.

The $H\alpha$ profile of an inactive MK standard of the appropriate spectral type (K0) is rotationally broadened and subtracted from the Hα profile at each phase in the timeseries for the purpose of measuring the chromospheric line flux. The true underlying photospheric absorption, however, is most certainly influenced by the temperature inhomogeneities on the stellar disk as are other absorption lines. We proceed under the assumption that the disk integrated equivalent width of the photospheric absorption is, to first order, preserved as the star rotates. This assumption is valid for nearly all of the photospheric lines and deviations from this should be small.

The residual line flux is then integrated within the $\pm 250\ km/s$ window bounded by the dotted vertical lines in Fig. 11. We cannot directly compare these quantities since each was computed relative to a different photospheric flux. We instead convert the residual line flux to an absolute line flux, $F_{H\alpha}$, by estimating the absolute stellar flux in the continuum at 6562.808Å at each phase in the timeseries. This is done in the following manner: Differential photometry (Sect. 2) and the image reconstruction give us an estimate of the stellar flux at 6562.808Å relative to an arbitrary zero-point. This relative flux is expressed as a fraction of the mean (or zero-point). The zero-point flux is then estimated using the Kurucz stellar atmosphere models (Kurucz 1994), interpolated to give the closest match to P1724. The Kurucz models have been found to be quite adequate spectrophotometric proxies of young cluster stars down to $\approx 5000\ K$ (Clampitt & Burstein 1997).

The resulting line fluxes at each rotational phase are listed in Table 3 and plotted in Fig. 12. While the chromospheric emission, as measured in $H\alpha$, does appear to be rotationally modulated, the peak of the emission does not coincide with the phase of spot transit. Since no IR excess emission has been detected in the star's SED (Fig. 6), we assume that there is no disk accretion contributing to the variability in $H\alpha$. More likely, the emission is chromospheric in origin and the variability should be explained in that context. The average line flux is typical of wTTS.

Using the solar analogy, we expect that plages in the upper atmosphere, seen as bright regions in $H\alpha$, might contribute to the rotational modulation of the line flux. Solar plages are found to be roughly co-spatial with underlying photospheric spots. If indeed plage regions are modulating the $H\alpha$ flux in P1724, they are not precisely co-spatial with photospheric active regions. However, we note that (a) the timeseries was taken over a period of seven stellar rotations; longer-term variations could be contaminating the flux measurements; (b) the variations seen during the third stellar rotation cannot be explained by measurement uncertainties alone; it appears that smaller amplitude flux variations do occur on timescales less than one stellar rotation; and (c) the $H\alpha$ profiles consist of both a narrow and broad emission component; the latter could be a consequence of the Stark effect and may indicate microflaring events (cf. Montes et al. 1997). Resolving the various contributions to the $H\alpha$ line flux and determining their spatial relation to photospheric active regions will require better time resolution and an independent analysis of the broad and narrow line contributions.

In the case of V410 Tau, Fernández & Miranda (1998) detected $H\alpha$ variability clearly modulated by rotation. They found very strong evidence from the line profiles, that this modulation is due to rotation. However, in the past, this modulation has not always been detected, sometimes the modulation is present, sometimes it is not detectable, although the spot appears to be stable over several years. Hence, while a spot may be stable for many years, plages are not, as discussed in Fernández & Miranda (1998). It might be possible to detect rotationally modulated $H\alpha$ emission in P1724 in the future, if it were to form sufficiently large plages.

In most of the high-resolution spectra which cover the 6000 to 6800Å region of the spectrum (Table 3; Figs. 10 e-h and 12), we detect narrow emission lines at ~ 6584Å, ~ 6300Å, and in the core of $H\alpha$. We identify the first two features as [NII] 6583.6 Å and [OI] 6300.3Å lines. The [OI] line falls at a constant heliocentric wavelength and is incompletely subtracted night sky emission (this line is not seen in the sky-subtracted ESO-3.6m CASPEC spectra). However, the [NII] and the narrow $H\alpha$ emission components, after heliocentric correction, are consistent with the rest velocity of P1724. These lines are too narrow to originate in the stellar atmosphere, but must be physically or dynamically related to P1724.

In the KPNO echelle slit spectra, the narrow $H\alpha$ component and the [NII] line are both spatially extended, but neither fill the 4 arcsec decker. The stellar continuum has a spatial FWHM of 0.91 arcsec near [NII], while the [NII] line has a FWHM of 1.01 arcsec. The $H\alpha$ line was not as well focussed, with spatial widths of 0.96 and 1.12 arcsec, respectively. The broad $H\alpha$ emission is no more extended than the stellar continuum. Uncertainties in the spatial width are about ± 0.025 arcsec. This suggests that these narrow emission lines arise in an extended region about half an arcsec in extent. There is a small nebulosity projected around P1724 (see, e.g. the POSS image in Fig. 3 of Preibisch et al. 1995); the narrow emission lines could arise in a portion of the nebulosity adjacent to the star. However, this emission cannot be wind, as P1724 is not that massive. Also, P1724 is not hot enough to excite nebula emission. The apparent ~ 0.1Å variation in the equivalent width of the [NII] line could be a combination of rotational modulations in the stellar continuum flux (which can account for only ~ 0.01Å variation in the

[9] The maximum value observed, namely W_λ(Li)$= 0.44$Å, would yield $\log\ N$(Li)$= 3.70 \pm 0.10$, which exceeds the primordial level.

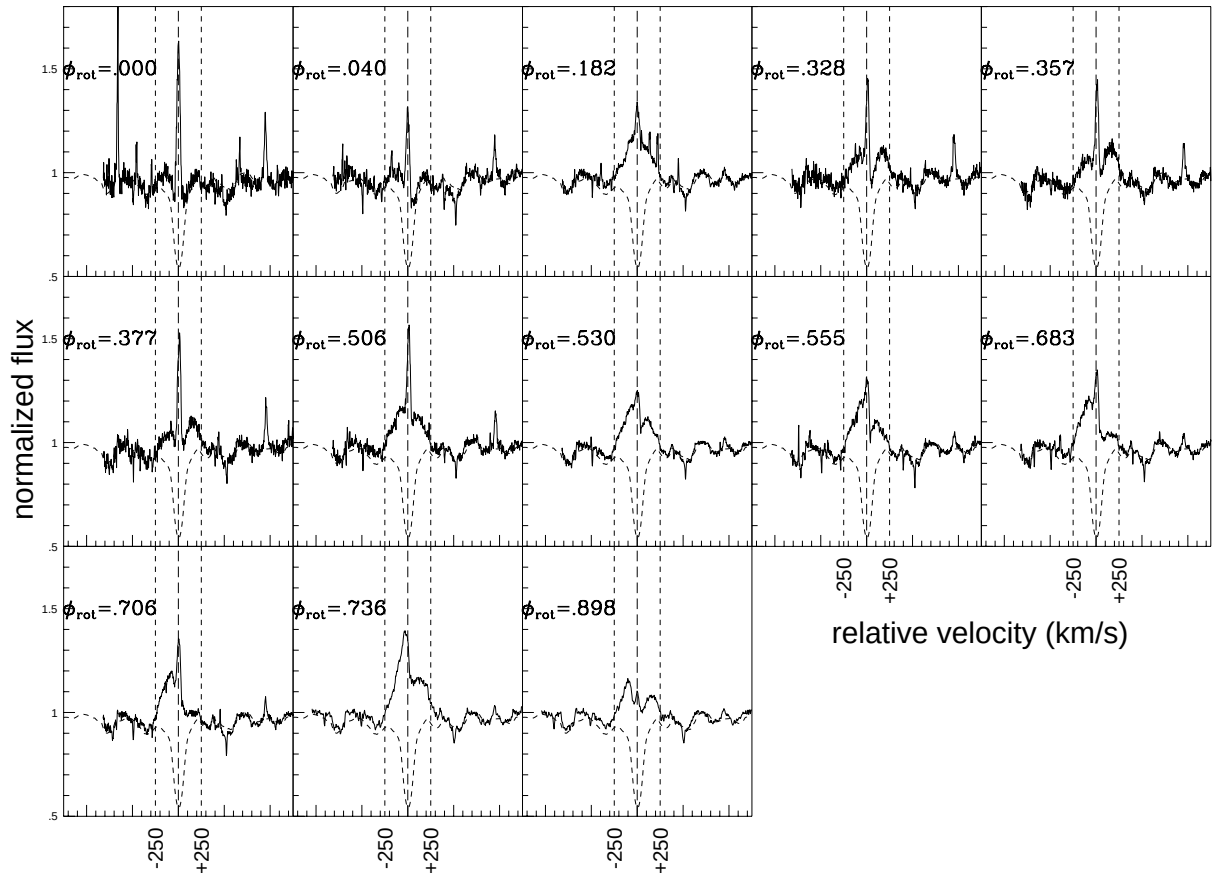

Fig. 11. $H\alpha$ line profiles of P1724. The figure shows the $H\alpha$ profiles extracted from the observations listed in Table 3, with the rotational phases indicated. The axes give the normalized flux versus the relative velocity (in $km\ s^{-1}$). Also shown are spectra of an inactive MK standard, rotationally broadened to match P1724, used to subtract residual spectra (see text for details)

equivalent width) and varying degrees of success in background subtraction.

Finally, we obtained an additional spectrum in the blue wavelength range on 20 Dec 1996 with the CAFOS at the Calar Alto 2.2m telescope, with a similar set-up (except using the blue grating G1) and reduction procedures as above. Fig. 13 shows this spectrum with Ca II H&K emission filling in the absorption lines. We estimate the equivalent widths of these lines to be $W_\lambda(K) = -0.14$Å and $W_\lambda(H) = -0.13$Å, rather typical for active young stars.

8. X-ray monitoring

Due to its position close to the Orion nebula, P1724 has been observed by ROSAT quite frequently: In 1990 it was observed with the ROSAT All-Sky Survey (RASS), and between 1991 and 1993 it was in the field of view of seven pointed ROSAT observations with both the Positional Sensitive Proportional Counter (PSPC) and the High Resolution Imager (HRI). For details on ROSAT and its instruments, we refer to Trümper (1983).

During the period 1 to 21 Sep 1995, J.-P. Caillault and coworkers performed a sequence of ten ROSAT HRI observations of the Trapezium region. The typical exposure time of each observation was 2 ksec, and the individual observations were separated by about two days. The X-ray sources in the Orion nebula cluster were monitored in this way for a period of 20 days (cf., Gagné et al. 1997 for the first results of this study). The details of all available ROSAT observations are given in Table 5.

We obtained the data for all of these observations from the ROSAT data archive and analyzed them with the Extended Scientific Software Analysis System (EXSAS, Zimmermann et al. 1995). With one exception, P1724 was clearly detected as an X-ray source in all these observations. The exception is pointing 200700, which had a very short exposure time of only 700 sec, and in which P1724 was located at a large off-axis angle of $47'$, where the sensitivity of the detector is significantly reduced. From this observation we determined an upper limit to the count rate of P1724.

In 1993 a deep ASCA observation of the Orion region was performed (Yamauchi et al. 1996). Again, P1724 was clearly detected as one of the brightest X-ray sources within the region observed.

8.1. The X-ray spectrum

Since Preibisch et al. (1995) describe the spectral analysis in detail, we only summarize here the results of the spec-

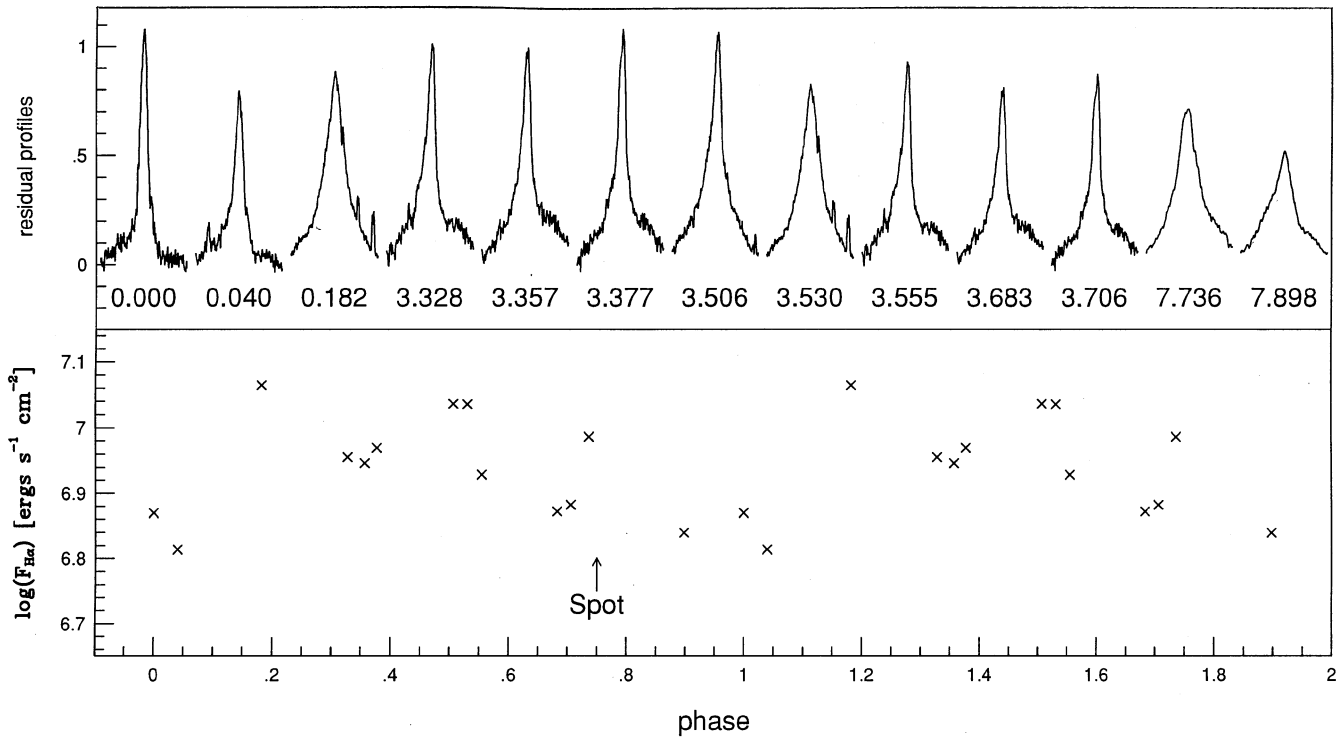

Fig. 12. Comparison of $H\alpha$ line flux and photospheric active regions. Plotted in the upper panel are the residual $H\alpha$ line profiles obtained by subtracting the rotationally broadened MK standard from the normalized line profiles of Fig. 11. The rotational phase of each profile is noted. The lower panel plots the absolute chromospheric line flux, $F_{H\alpha}$, versus rotational phase. The phase of primary spot transit is also indicated

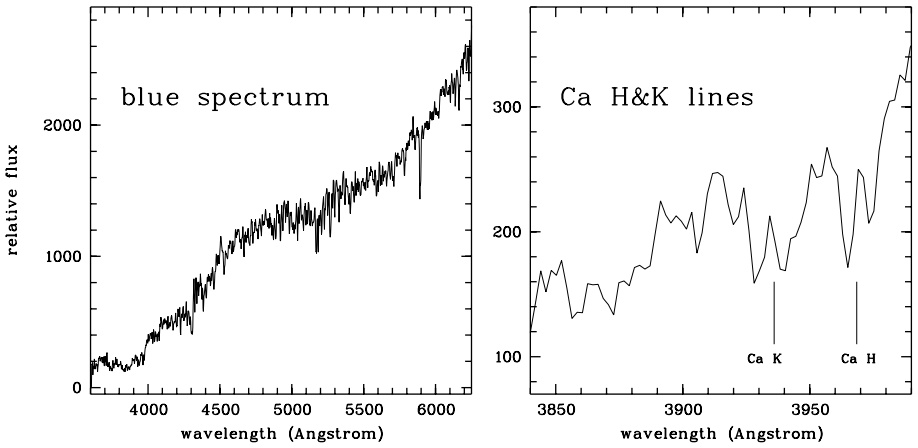

Fig. 13. Low-resolution spectrum of P1724 in the blue region. The full spectrum is shown in the left panel (flux versus wavelength), and an enlargement of the Ca H&K lines is seen on the right

tral fits. The X-ray spectrum of P1724 was extracted from PSPC observation 200151. In this observation the count rate of P1724 showed no significant variations and thus we are confident that these data yield the quiescent X-ray spectrum. An isothermal plasma model clearly failed to reproduce the spectrum. A two-temperature model gave an acceptable fit with $N_{\rm H} = 0.94^{+0.25}_{-0.14} \times 10^{21}\,{\rm cm}^{-2}$, $\log\ (T_1/{\rm K}) = 6.9^{+0.1}_{-0.2}$, and $\log\ (T_2/{\rm K}) = 7.5^{+0.2}_{-0.1}$.

The spectrum could be equally well fitted by a model with a continuous temperature distribution in the form of a power law up to a maximum temperature (cf. Schmitt et al. 1990 or Preibisch 1997 for a discussion of this model). The fit with this model gave $N_{\rm H} = 0.96^{+0.23}_{-0.20} \times 10^{21}\,{\rm cm}^{-2}$, a maximum temperature of $\log\ (T_{\rm max}/{\rm K}) = 8.0^{+0.4}_{-0.2}$, and a power-law exponent of $\alpha = 1.1^{+0.5}_{-0.3}$.

From their deep ASCA observation Yamauchi et al. (1996) also extracted spectra for P1724. A simultaneous two-temperature fit to the SIS and GIS spectra yielded $N_{\rm H} = 1.1^{+0.9}_{-0.6} \times 10^{21}\,{\rm cm}^{-2}$, $\log\ (T_1/{\rm K}) = 6.9^{+0.1}_{-0.1}$, $\log\ (T_2/{\rm K}) = 7.5^{+0.1}_{-0.1}$, which agrees very well with the results of our fit to the ROSAT spectrum.

From the spectral parameters of the fits one may calculate the X-ray luminosity in the 0.1 to 2.4 keV ROSAT band. The X-ray luminosity computed for the two-temperature model agrees very well with that for the power law temperature distribution model. Assuming a distance of 460 pc, we find $L_{\rm X} = (6.8 \pm 0.7) \times 10^{31}$

Table 5. ROSAT pointed observations of P1724. ROR is the ROSAT observation number, the prefix 'P' indicates observations with the PSPC detector, the prefix 'H' those with the HRI detector. We list the dates of the start and end of the observation period, the exposure times τ, and the mean count rates $<cr>$ for each observation. For the sequence of monitoring observations we list the minimum and maximum count rates.

ROR	start/stop date	τ [ksec]	$<cr>$ [cnts/sec]
P200151	14/18 Mar 91	9.7	0.163 ± 0.005
H200006	20/24 Mar 91	11.4	0.059 ± 0.002
H200500-1	02/03 Oct 91	28.1	0.049 ± 0.010
P200700	26/27 Feb 92	0.7	< 0.130
H200500-2	22/22 Mar 92	1.0	0.043 ± 0.022
H200500-3	14/15 Sep 92	18.0	0.055 ± 0.010
P201030	26/28 Feb 93	7.9	0.057 ± 0.003
H201784 - H201785 H201787 - H201794	01/21 Sep 95	~ 2	min: 0.042 max: 0.110

erg/sec. This is the quiescent X-ray luminosity during observation 200151 in March 1991. This observation was also used to determine the conversion factor between count rate and X-ray luminosity for other ROSAT observations.

8.2. X-ray variability

We extracted background-corrected lightcurves for P1724 from all ROSAT observations and analyzed them for signs of variability. While most of the lightcurves show only small-amplitude irregular variability, significant enhancements of the count rate can be found in the light curve extracted from the RASS data and from the HRI observation 200500.

The large flare discussed in detail by Preibisch et al. (1995) occurred during the third part of observation 200500 in Sep 1992. Since Preibisch et al. (1995) assumed a distance of 500 pc, the energetics of this flare have been slightly overestimated. However, even with an assumed distance of 460 pc the total flare energy radiated in the ROSAT X-ray band is $\approx 4 \times 10^{37}$ erg, and this is still one of the most energetic flares ever observed on a star. Only the IR protostar IRS 43 (=YLW 15) has been caught by ROSAT HRI at an even more energetic flare (Grosso et al. 1997).

During the RASS observations in 1990 (Fig. 14a) and also during the first part of observation 200500 in Oct 1991 (Fig. 14b), the X-ray lightcurve shows systematic enhancements of the count rate lasting for ~ 20 hours. In both events the maxima are not narrow and rise and decay times are approximately equal, which is quite atypical for a flare. The variations might indicate rotational modulation (Neuhäuser et al. 1995b); however, this would imply a rotation period of ~ 40 hours, clearly inconsistent with the observed photometric period of 5.7 days (cf. Sect. 2).

An alternative interpretation might be a flaring event which occurred on the back side of the star shortly (compared to the rotation period) before the flaring plasma became visible at the stellar limb. Two effects are relevant: (1) The flaring plasma cools, so that its X-ray emission decreases, but (2) more X-ray emitting plasma gradually becomes visible as it rotates into view. These two effects together might qualitatively account for the observed light curves (cf., Casanova 1994). During the X-ray flare of Sep 1990, the rotational phase at the beginning of

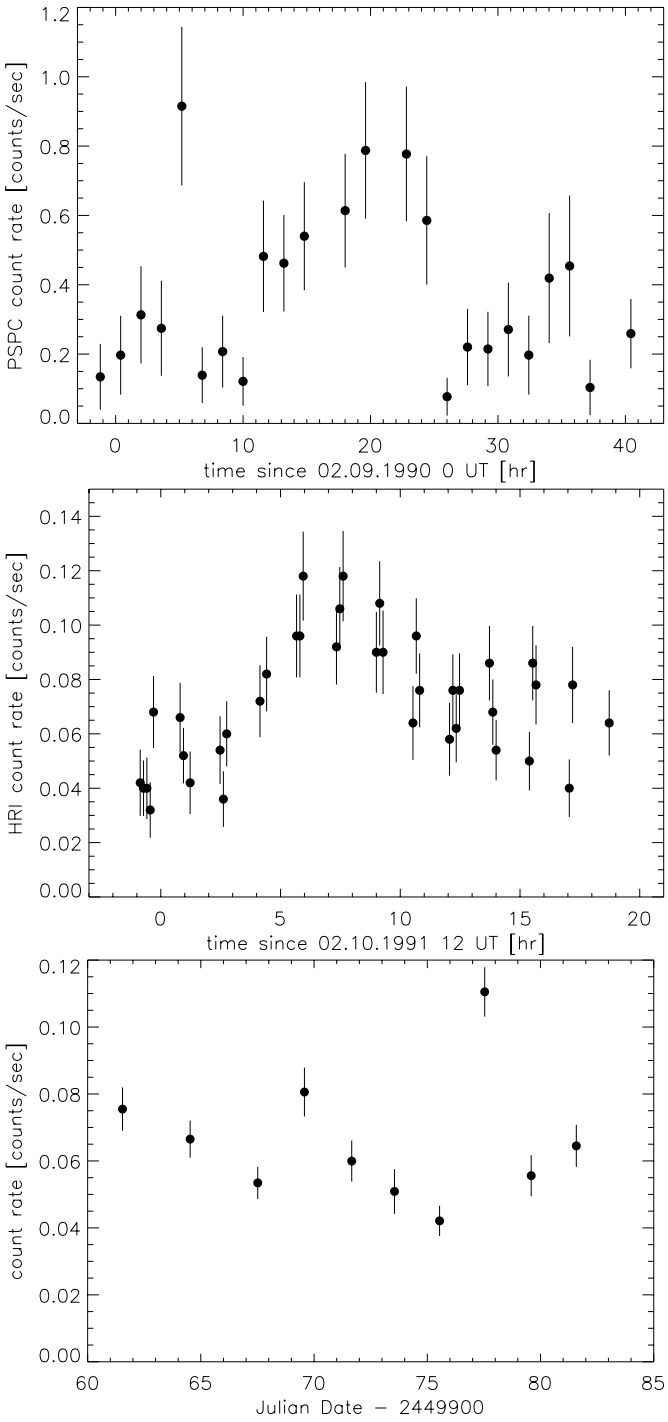

Fig. 14a–c. X-ray lightcurves. We show ROSAT count rate versus time of observation. **a** ROSAT All Sky Survey (upper panel), **b** first part of HRI observation 200500 (middle panel), and **c** HRI observations in Sep 1995 (lower panel)

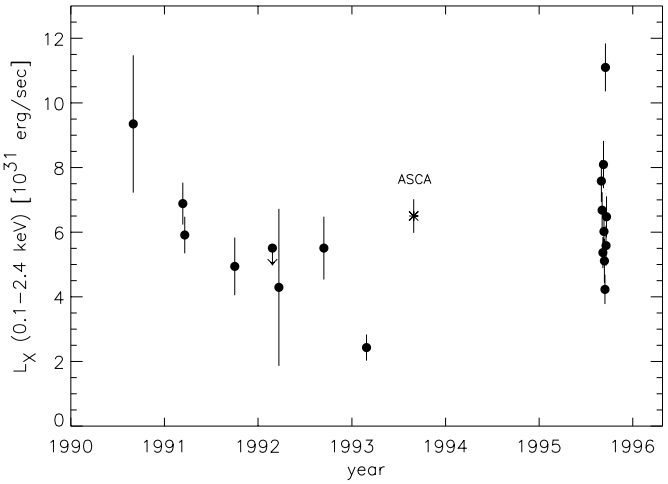

Fig. 15. Long term X-ray variation. We show X-ray luminosity in 10^{31} erg/sec versus observation date given in years. The first data point is from the ROSAT All-Sky Survey. The upper limit from observation 200700 is marked by an arrow. The X-ray luminosity reported by Yamauchi et al. (1996) for the (0.5 – 10 keV) ASCA band was transformed to the ROSAT band (0.1 – 2.4 keV) by using the spectral parameters from the 2T fit

the flare event was 0.013; and the beginning of the flare in Oct 1991 took place at phase 0.612. Hence, both flares took place roughly midway between minimum and maximum visible light, somewhat closer to minimum. Assuming that the X-ray flares originated at or near the dark spot area, this suggests that the flares may have occurred rather close to the limb of the star. We shall investigate this scenario quantitatively in more detail elsewhere (Neuhäuser et al., in preparation).

The lightcurve constructed from the HRI monitoring observations in 1995 is shown in Fig. 14c. While the variations appear quite smooth, the lightcurve cannot be described as a sinusoidal variation. Neither a period of 40 hours nor 5.7 days can reproduce the observed lightcurve. Hence, we do not see any evidence for rotational modulation in the X-ray data.

The data point for observation 201792 (JD 2449977) shows a significantly higher count rate than in the other observations of the series. A closer look at the lightcurve within observation 201792 indicates a decreasing count rate. However, due to the short exposure time of this observation (2.2 ksec) no meaningful analysis of this lightcurve is possible. Most probably P1724 showed another flare a few hours before the beginning of observation 201792.

The ASCA lightcurve presented in Yamauchi et al. (1996) shows variability of a factor of about 2. One data point in their binned lightcurve is roughly a factor of 3 above the mean, but no flare-like decay can be seen.

Finally, we used all available data to construct a long term X-ray lightcurve for P1724, covering approximately 5 years (Fig. 15). The variation in X-ray luminosity between 1990 and 1993 by about a factor of 2 is consistent with the variation found from the monitoring in Sep 1995 on a shorter time-scale.

8.3. Discussion of the X-ray properties

The mean quiescent X-ray luminosity of P1724 is $\sim 7 \times 10^{31}$ erg/sec. This is quite high, even for an X-ray luminous TTS. By comparison with the X-ray luminosities derived by Gagné et al. (1995) for the TTS in the Orion nebula cluster, P1724 seems to be the most X-ray luminous TTS in Orion, surpassed only by the O and B stars. However, in the sample of Gagné et al. (1995) there are five stars of spectral type G or K with X-ray luminosities between 3 and 6×10^{31} erg/sec. Thus we conclude that the X-ray luminosity of P1724 is extreme but still consistent with that of the other X-ray luminous TTS in the Orion nebula cluster.

Using the bolometric luminosity of $\approx 49\ L_{\odot}$ from Sect. 5, we find a ratio $L_{\rm X}/L_{\rm bol} \approx 1.3 \times 10^{-3}$. This is in the typical range as reported by Gagné et al. (1995) for the most X-ray luminous G and K stars (between 3×10^{-4} and 2×10^{-3}). Similarly, the X-ray surface flux of $F_{\rm X} \simeq 1.3 \times 10^{7}$ $erg/sec/cm^2$ is in the typical range for X-ray active TTS, which is 0.03 to 2.5×10^{7} $erg/sec/cm^2$ (cf., Neuhäuser et al. 1995a, Preibisch 1997).

Gagné et al. (1995) thoroughly investigated the variability of the X-ray sources in the Orion nebula cluster. They found that at least 1/4 of the TTS show significant X-ray variability on time scales of about one year with typical amplitudes of factors of 2 to 6. Thus, the X-ray variability displayed by P1724 is quite typical for TTS. The variability cannot be explained as rotational modulation. This means that the X-ray emission is not dominated by a single active region or by a dense group of active regions associated with the predominant spot group. The X-rays probably originate from a multitude of active regions distributed widely on the stellar surface.

We conclude that the X-ray properties of P1724 are extreme in some aspects, but nevertheless are consistent with those of other X-ray bright TTS in the Orion nebula cluster.

9. Proper motion

Several proper motion studies of the Trapezium cluster as a whole have been performed, including star P1724 (see Table 6 for details). With only one exception (Fallon 1975) all studies were carried out in a relative rectangular x-y coordinate system, with the zero-point of the proper motions defined by the Trapezium member stars included in the different investigations.

Nearly all of these studies find that the proper motion of P1724 in right ascension (or x) is very close to the cluster mean. The proper motion in declination (or y), on the other hand, is fairly larger than the observed velocity dispersion which is believed to be smaller than 1 mas/yr, corresponding to $\approx 2\,km\,s^{-1}$ at a distance of 460 pc.

Depending on the membership criterion applied, conclusions regarding the membership of P1724 to the Trapezium cluster differ from author to author: The calculated membership probabilities based on the proper motion range from 0 to $97\,\%$, reflecting the fact that the proper motion of P1724 is very close to the boundary chosen to separate members and non-members.

Table 6. Proper motions of P1724. For each study in the first column the table lists the proper motion and mean errors in x and y coordinates relative to the mean motion of the Trapezium cluster. The only absolute proper motions are those by Fallon (FK4 system) and STARNET (HIPPARCOS system). The next columns show the epoch difference, the number of stars investigated, the number of members, and the probability of membership of P1724 to the Trapezium cluster.

	μ_x [mas/yr]	μ_y [mas/yr]	ΔE [yr]	N_{total}	$N_{members}$	P [%]
Parenago 1954	-1.5 ± 1.2	4.7 ± 1.2	50	2983	634	97 (1)
Strand 1958	-0.8 ± 1.2	10.7 ± 1.2	50	224	154	0 (2)
Fallon 1975 (3)	-8.1 ± 0.4	5.6 ± 0.4	50	113	~ 100	
Jones & Walker 1988	-1.2 ± 1.3	-0.2 ± 1.2	20	1053	~ 900	42
Van Altena et al. 1988	-1.4 ± 0.14	7.1 ± 0.13	77	73	49	0
McNamara et al. 1989	0.38 ± 0.40	8.31 ± 0.49	76	640	249	0
Tian et al. 1996	-1.3 ± 0.2	6.6 ± 0.4	83	333	181	0
STARNET (3)	1 ± 3.5	5 ± 3.5	80			

Remarks: (1) P calculated by McNamara & Hüls (1983). (2) P calculated by McNamara (1976). (3) Fallon (1975) and STARNET give μ_α and μ_δ.

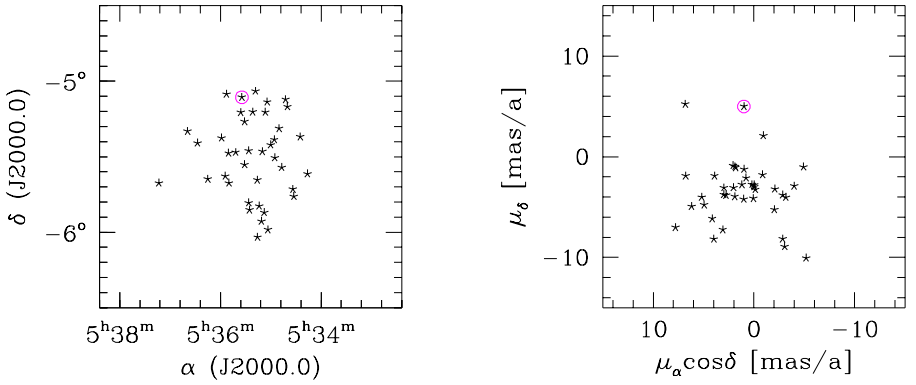

Fig. 16. Position and proper motion. We present the positions and proper motions of the 39 most probable members in the central part of the Trapezium cluster which could be identified in STARNET. The proper motions have been slightly randomized (0.25 mas/yr) in order for overlapping points to show in the figure (proper motions in STARNET are given as integers in units of milli arc sec per year. P1724 is marked with a circle in both diagrams. It is located north of the Trapezium and it moves north relative to the Trapezium

We discuss here a new proper motion from the STARNET Catalogue (Röser 1996), a proper motion catalogue based on a comparison between plates from the Astrographic Catalogue and the Guide Star Catalogue (GSC 1.2, Röser et al. 1996), with an epoch difference of ≈ 80 yrs. It contains 4.3 million stars, and provides proper motions in an absolute system with an accuracy of ≈ 5 mas/yr. For this study we have selected all stars from the membership list of Parenago (1954), which show no significant offset from the cluster neither in the position nor in the proper motion diagram.

For the center of the Trapezium cluster we adopt the position of θ^1 Ori, i.e. $\alpha_{2000} = 5^h35^m15\overset{s}{.}00$ and $\delta_{2000} = -5°23'29\overset{''}{.}3$. Hence, P1724 is located about 15′ from the center of the Trapezium. The mean proper motion of the cluster, using STARNET data converted to the absolute HIPPARCOS system for 38 stars, i.e. all probable members excluding P1724, is $\mu_\alpha \cdot \cos\delta = +1.2 \pm 3.3$ mas/yr and $\mu_\delta = -3.6 \pm 2.8$ mas/yr, while the proper motion of P1724 is $\mu_\alpha \cdot \cos\delta = +1 \pm 3.5$ mas/yr and $\mu_\delta = +5 \pm 3.5$ mas/yr. This indicates that P1724 is moving north relative to the cluster. Although we see a few more outliers in the proper motion diagram (Fig. 16), the cluster as a whole is not expanding. Not only is the proper motion of P1724 off by $\sim 3\sigma$ from the mean, but the star is also located north of the cluster and is moving north relative to the cluster, so that it seems very likely that it has been ejected.

The errors in STARNET are on average larger than those in relative proper motion studies due to possible errors in the parameters involved in the transformation to the absolute system. But in contrast to the relative studies, proper motions in an absolute astrometric system can provide information on the overall expansion or rotation of a cluster. Indeed, Strand (1958) argued for an overall expansion of the Trapezium cluster, although Vasilevskis (1971) expressed doubts about this conclusion. In contrast to Strand (1958), Fallon et al. (1977) found evidence for a contraction of the Trapezium cluster from an analysis of the proper motions of Fallon (1975) in the FK4-system. From our analysis of the STARNET proper motions, we find no evidence for expansion, contraction, nor rotation of the cluster.

To compare the 3D space motion of P1724 with the mean motion of the Trapezium stars, we note that the mean RV of the Trapezium stars is $+25.5\ km/s$, with a 2 σ scatter of $4\ km/s$ (Hartmann et al. 1986). In Sect. 3 we determined the mean radial velocity of P1724 to be $+23\ km/s$.

We conclude from the observed kinematics of P1724 relative to the Trapezium cluster that (a) there is no difference in the mean radial velocity and proper motion in right ascension between P1724 and the cluster mean, and (b) there is a clear difference in the proper motion in declination of about 9 mas/yr, or $20\ km\ s^{-1}$ at a distance of 460 pc. Together with its position 15 arc min north of the center of the Trapezium (Fig. 16), this is

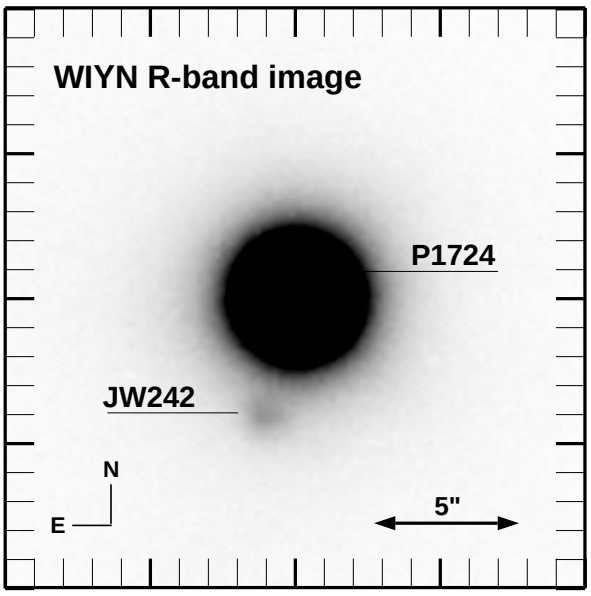

Fig. 17. R–band image of P1724. One of our WIYN images in the R band showing P1724 and the faint star JW 242, about 4 arc sec to the south. The exposure time was 5 seconds. The faint annulus seen in our WIYN R band image around P1724 is due to the PSF of the instrument

compatible with the scenario that P1724 has been ejected from that cluster $\approx 10^5$ yrs ago.

10. R- and K-band imaging

Our spectroscopic observations (Sect. 3) show no evidence for companions to P1724 with periods up to ~ 500 days. In order to search for much wider companions, we have performed R-band imaging with the WIYN 3.5m telescope at KPNO. We used the S2KB instrument with a STIS 2048×2048 pixel CCD, and a resolution of 0.195 arc sec per pixel. Data reduction was carried out with the GaussFit package (Jeffries et al. 1991) following Brandner et al. (1996). For details on the observations and data reductions, see Sterzik et al. (1997).

We obtained four exposures of P1724 on 19 Nov 1995 with 1 to 10 sec integrations, and a seeing of ~ 1 arc sec. One of our images is displayed in Fig. 17, and clearly shows a star ~ 4 arc sec south of P1724. This object is known as JW 242, star number 242 in Jones & Walker (1988), for which those authors give $V \approx 14$ mag. The brightness difference between P1724 and JW 242 is $\Delta R \simeq 5$ mag in our WIYN image. Jones & Walker (1988) give $\Delta V \simeq 5$.

The proper motion study by Jones & Walker (1988) is the deepest done so far, and their proper motion of JW 242 is the only one published. They list $\mu_x = -7.8 \pm 1.0$ and $\mu_y = +9.8 \pm 2.1$ for JW 242, which is $> 3\ \sigma$ deviant from the proper motion they list for P1724, namely $\mu_x = -1.2 \pm 1.3$ and $\mu_y = -0.2 \pm 1.2$ (all in mas/yr). From the positions of these two stars given by Jones & Walker (1988), we estimate the position angle to be 155° and the separation to be ~ 4.2 arc sec. Since the epoch difference between the Jones & Walker image and our WIYN image is about 45 years, and given the proper motions, the position angle of this pair should now (i.e. at the time of our WIYN observation) be $\sim 165^\circ \pm 1^\circ$, unless there is orbital motion. The measured position angle in our WIYN image is $\sim 164.5^\circ$. The excellent agreement with the prediction from proper motions further supports the conclusion that the pair is only a chance projection, and not a physical system.

In order to search for companions that are even closer, we used the speckle interferometry technique. The observations were carried out on 22 Nov 1997 at the 3.5m telescope on Calar Alto, using the near-IR camera MAGIC (Herbst et al. 1993) in the K-band at $2.2 \mu m$. The modulus of the complex visibility (i.e. the Fourier transform of the object brightness distribution) was determined from power spectrum analysis, the phase was computed using the Knox-Thompson algorithm (Knox & Thompson 1974) and from the bispectrum (Lohmann 1983).

We found no evidence for a companion. To quantify this statement, we computed the maximum brightness ratio of a companion that could be hidden in the noise of the data to obtain upper limits for the brightness of an undetected companion as function of the separation. For details of this procedure, see Leinert et al. (1996). We can exclude companions brighter than $10\ \%$ of the primary in K, corresponding to a magnitude difference of $\Delta K = 2.5$ mag, at all separations larger than 0.13 arc sec, the diffraction limit of the telescope. For separations larger than 0.2 arc sec, we can even exclude companions brighter then $4\ \%$ of the primary, i.e. $\Delta\ K = 3.5$ mag.

11. Discussion and conclusions

We have obtained ~ 200 optical and IR photometric measurements and ~ 60 high- and low-resolution spectra of the very active young star P1724 in Orion with the following results:

1. The rotational period is confirmed to be 5.7 days, based on new photometric VRI monitoring and a re-analysis of other photometry from the literature.
2. The mean heliocentric radial velocity is $+23\ km\ s^{-1}$, consistent with membership to the Orion association.
3. The variability in both the photometric and radial velocity data with the same period and the same phase, which has apparently been stable for 30 years, can be explained by the presence of dark surface features, reconstructed from Doppler imaging techniques applied to our high-resolution spectra. The magnetic field is estimated from equipartition to be $\sim 1.9\ kG$.
4. The spectral energy distribution is consistent with a spectral type K0, with no evidence for IR or UV excess. The derived radius is $\sim 9\ R_\odot$ assuming a distance of $460\ pc$. The bolometric luminosity is $L_{bol}\ \simeq 49\ L_\odot$. From its locus in the H-R diagram and theoretical tracks and isochrones, its mass is estimated to be $\sim 3\ M_\odot$, and its age is $\sim 2 \times 10^5$ yrs.
5. The surface gravity is $\log g \simeq 3$, both from the distance-dependent locus of the star in the H-R diagram and also from our direct distance-independent measurements based on high-resolution spectra.
6. The projected rotational velocity from our high-resolution spectra is $v \cdot \sin i\ =\ 71\ km\ s^{-1}$. From this and its other

physical parameters, we estimate the inclination to be $\sim 62°$. Since K-type post-MS giant stars all rotate much slower (Gray 1989) and show less lithium, P1724 is a pre-MS star.

7. The $H\alpha$ equivalent width is variable, with $W_\lambda(H\alpha) \simeq 0.7$ to 3.5Å. P1724 also shows other activity indicators including strong Ca II H &K emission lines and variable X-ray emission.
8. The equivalent width of the lithium 6708Å absorption line is found to be modulated by rotation, and is larger when the spot is in front. The unspotted star has W_λ(Li)$\simeq 0.34$Å (from high-resolution spectroscopy), corresponding to an abundance of $\log\ N$(Li)~ 3.2.
9. There are no indications of any physically bound visual companions down to $\Delta R \simeq 7$ mag and ~ 1 arc sec separations, nor any companions down to 0.13 arc sec and $\Delta\ K = 2.5$ mag. We cannot completely rule out the presence of a closer spectroscopic companion, perhaps even a brown dwarf, which could conceivably be causing part of the observed RV variation. JW 242 and P1724 form a $4''$ visual pair, but show different proper motions, so that they are probably not gravitationally bound; if they were located at about the same distance, JW 242 – being ~ 5 mag fainter than P1724 – might also be a brown dwarf.
10. The proper motion of P1724 indicates that it is moving north relative to the Trapezium, and its 3D space motion suggests that it may have been ejected from the Trapezium $\approx 10^5$ yrs ago.

From optical follow-up observations of unidentified X-ray sources found in the RASS, large numbers of wTTS have been discovered in and around Orion and other SFRs (Alcalá et al. 1996; see also the recent review by Neuhäuser (1997) with more references therein). One possible explanation for the presence of young wTTS located several degrees from active star forming clouds is the run-away TTS (raTTS) hypothesis. According to Sterzik & Durisen (1995), young stars can be ejected when formed in multiple protostellar systems, so that they would move with high velocities and could be found far away from their birth places. Such raTTS should preferentially be either single TTS or close binaries, since tight binaries do not easily break apart in typical encounters. Depending on the ejection geometry, raTTS may show a radial velocity and/or proper motion different from the mean value of their parent association, i.e., may seem to have kinematics inconsistent with membership. The evidence discussed above supports the conclusion that P1724 is indeed a raTTS.

Ejected TTS may lose at least part of their circumstellar material during the encounter (e.g., Brandl & Sterzik 1997), consistent with the fact that we detect no IR excess emission in the SED of P1724. However, we also note that Hillenbrand et al. (1998) found a gradient in the fraction of stars which show near-IR excess as a function of projected radius from the center of the Trapezium, even after correcting for the falloff in membership probability with increasing cluster radius. Furthermore, there appears to be a gradient in the mean accretion rates with cluster radius, where they are higher in the center than in the outer parts of the cluster. Their interpretation is that the higher stellar density in the interior causes enhanced disk accretion rates and, consequently, that more stars with near-IR excess are detected than one would detect if the mean accretion rates were lower (Hillenbrand et al. 1998). At a projected radius of $15'$ from θ^1 Ori, they found a minimum disk fraction of $\sim\ 30\ \%$, and more disks further inwards. We can speculate that the lower disk fraction and the smaller near-IR excesses found with increasing distance from the Trapezium center may partly be due to a some contribution of raTTS, which have lost their circumstellar material during the encounter.

In many regards, P1724 appears to be similar to P1540, studied in detail by Marschall & Mathieu (1988): Both stars show RV consistent with membership, but inconsistent proper motion; they are located just outside the Trapezium cluster and show 3D space motion pointing away from the Trapezium. Both might have been ejected from the cluster $\sim 10^5$ years ago, in both cases easily within the respective ages of the stars. P1540 is a double-lined spectroscopic binary, but its separation is small enough, so that the encounter would not disrupt the binary. These two stars appear to be very good examples for the raTTS hypothesis.

Kroupa (1995) has suggested that low-mass stars can be ejected dynamically from very dense clusters such as the Trapezium by mutual interactions. According to both Kroupa (1995) and Sterzik & Durisen (1995), there is in fact some chance that even stars as massive as P1724 can be ejected. Although it is much more likely for lower-mass stars to be ejected, more massive stars can be more easily detected because they are much more luminous.

The rather large projected rotational velocity and the rather long rotational period imply that P1724 is seen not far from equator-on. We derived above an inclination angle of $i = 62°$, from which $\sin i = 0.88$. Given the observational constraints, the minimum possible value of the radius assuming $\sin i = 1$ is $\sim\ 8\ R_\odot$. This in turn would be consistent with a distance of $\sim\ 363\ pc$, which we consider as a lower limit. Although P1724 does not show any IR excess, its apparent extinction of $A_V\ =\ 1.6$ mag is rather large for a naked wTTS. However, on optical images, one can see a small nebulosity (cloudlet) at the location of P1724, and it is very likely that this nebula is the reason for the large extinction. P1724 is located inside or behind the nebula.

According to our data, the local-standard-of-rest (LSR) radial velocity of P1724 is $(8.0 \pm 1.0)\ km/s$, while the LSR velocity of the nebula at its location is slightly different, namely $11.0 \pm 0.2)\ km/s$ (Maddalena et al. 1986), computed for the material at the location of P1724 using the original Maddalena et al. data by T. Dame (priv. comm.), but the Maddalena et al. beam was not directly pointed towards P1724. However, the RV of P1724 is not different from the RV obtained (above) for the [NII] line, which probably originated in this nebula. Hence, we cannot conclusively confirm, whether or not P1724 and the nebula are co-moving in the radial direction. Yet, from the proper motion of P1724 and the Trapezium stars, we know that P1724 is moving with a large velocity relative to the Trapezium and the Orion clouds. Hence, we conclude that P1724 is currently

crossing through this nebula, although they may have the same RV. Unfortunatelly, the proper motion of the nebula is unknown and difficult to measure.

It is also possible that the nebula itself, or even both the nebula and the star together, were ejected from the Trapezium. Gorti & Bhatt (1996) argue that small neabulae can be ejected from molecular cloud regions by cloud-cloud interaction. This might have happened to the nebula we see near P1724, but we cannot measure the proper motion of the cloud to check this. P1724 could have formed in the nebula some time after the ejection of the nebula, or the nebula and the star could have been ejected together, or the cloud and the star just happen to be located at the same position. However, all these hypotheses appear to be very unlikely.

Because this small nebula is located close to the Trapazium and because its RV is not different from the mean RV of the Orion clouds and stars, this nebula is most likely part of the Orion molecular cloud complex, which can be taken as another indication for the fact that the distance of P1724 cannot be much smaller than the distance towards the Orion SFR. We also stress again that both a distance-dependent gravity measurement (namely the location in the H-R diagram) and a distance-independent gravity measurement (namely fitting our high-resolution spectra) yield the same surface gravity, so that the distance assumed cannot be far off.

We conclude that P1724 is a very young, relatively massive weak-line T Tauri star without UV or IR excess emission located at the distance of the Orion clouds, and it may well be a good example of a run-away T Tauri star ejected from the Trapezium cluster $\approx 10^5$ years ago.

Acknowledgements. We are grateful to F. Bertoldi, M. Fernández, E. Guenther, L. Hillenbrand, G. Morfill, S. Röser, and H. Zinnecker for useful discussion about P1724 and also would like to thank the referee, G. Tagliaferri, who has helped us a lot in improving the paper. M. Gagné originally pointed our interest to P1724. We acknowledge the supporting staff at the many different telescopes used in this research. SJW would especially like to thank the observers who took data at Stony Brook. GT wishes to acknowledge the help of the CfA observers at Oak Ridge, the Whipple Observatory, and the MMT. We are grateful to S. Melchert for the reduction of the *RW* photometry data set. R. Durisen provided the possibility to observe P1724 at WIYN and participated in the observing run. T. Dame computed for us the velocity of the cloud material near the location of P1724. G. Cutispoto kindly provided his photometric data of P1724. Also, we are grateful to the Principle Investigators of the ROSAT observations used in this research. The ROSAT project is supported by the Max-Planck-Gesellschaft and Germany's federal government (BMBF/DLR). APH acknowledges the support of NSF grant AST-9315115; RN, MFS, TP, SF, and RK acknowledge grants from the Deutsche Forschungsgemeinschaft (Schwerpunktprogramm 'Physics of star formation'). SJW was supported through NASA contract NASB-39073. NMSB is grateful to the Dep. of Astrofisica, Rio de Janeiro, and the Fundacao de Amparoa do Estado.

References

Alcalá J.M., Terranegra L., Wichmann R., Chavarría C., Krautter J., 1996, A&AS 119, 7
Alcalá J.M., Krautter J., Covino E., et al., 1997, A&A 319, 184
Alcalá J.M., Chavarría-K. C., Terranegra L., 1998, A&A 330, 1017
Barnes T.G. & Evans D.S., 1976, MNRAS 174, 489
Basri G., Marcy G., Valenti J., 1992, ApJ 390, 622
Beckwith S.V.W., Sargent A.I., Chini R.S., Güsten R., 1990, AJ 99, 924
Bouvier J., Cabrit S., Fernández M., Martín E.L., Matthews J.M., 1993, A&A 272, 176
Brandner W., Alcalá J.M., Kunkel M., Moneti A., Zinnecker H., 1996, A&A 307, 121
Brandl A. & Sterzik M.F., 1997, 'Multiple star-disk encounter'. In: *Astronomische Gesellschaft Abstract Series* Vol. 13, 17
Breger M., Gherz R.D., Hackwell J.A., 1981, ApJ 248, 963
Brown A.G.A., DeGeus E.J., de Zeeuw P.T., 1994, A&A 289, 101
Brun A., 1934, Publ. Obs. Lyon 1, No. 12
Cabrit S., Edwards S., Strom S.E., Strom K.M., 1990, ApJ 354, 687
Casanova S., 1994, PhD Thesis, L'Universite Paris IV
Clampitt L. & Burstein D., 1997, AJ 114, 699
Cohen M. & Kuhi L.V., 1979, ApJS 41, 743
Covino E., Alcalá J.M., Allain S., et al., 1997, A&A 328, 187
Cutispoto G., Tagliaferri G., Pallavicini R., Pasquini L., Rodonó M., 1996, A&AS 115, 41
D'Antona F. & Mazzitelli I., 1994, ApJ Suppl. 90, 467
Donati J.-F., Semel M., Carter B.D., Rees D.E., Cameron A.C., 1997, MNRAS 291, 658
Elias J.H., Frogel J.A., Matthews K., Neugebauer G., 1981, AJ 87, 1029
Fallon F.W., 1975, PhD Thesis, Florida University, Gainsville
Fallon F.W., Gerola H., Sofia S., 1977, ApJ 217, 719
Fernández M. & Miranda L.F., 1998, A&A, in press
Forestini M., 1994, A&A 285, 473
Gagné M., Caillault J.-P., Stauffer J.R., 1995, ApJ 445, 280
Gagné M., Caillault J.-P., Stauffer J.R., Linsky J.L., 1997, ApJ 478, L87
Genzel R. & Stutski J., 1989, ARAA 27, 41
Gorti U. & Bhatt H.C., 1996, MNRAS 278, 611
Gray D.F., 1989, ApJ 347, 1021
Grosso N., Montmerle T., Feigelson E.D., et al., 1997, Nature 387, 56
Guenther E. & Emerson J., 1996, A&A 309, 777
Hall D.S. & Busby M.R., 1990, 'Starspot lifetimes'. In: C. Ibanoglu (Ed.), *Active Close Binaries*, NATO ASI Series Vol. 319, Kluwer, Dordrecht, 377
Hartmann L.W., Hewett R., Stahler S., Mathieu R.D., 1986, ApJ 309, 275
Hatzes A.P., 1995, ApJ 451, 784
Herbig G.H. & Bell K.R., 1988, Lick Obs. Bull. 1111 (HBC)
Herbst T.M., Birk C., Beckwith S.V.W., Hippler S., McCaughrean M.J., Mannucci F., Wolf J., 1993, Proc. SPIE 1946, Fowler, A.M. (ed.), 605
Hillenbrand L.A., Strom S.E., Calvet N., et al., 1998, in preparation
Jeffries W.H., McArthur B., McCartney J.E., 1991, BAAS 23(2), 997
Johns-Krull C.M., 1996, A&A 306, 803
Johns-Krull C.M. & Hatzes A.P., 1997, ApJ 487, 896
Jones B.F. & Walker M.F., 1988, AJ 95, 1755
Joncour I., Bertout C., Menard F., 1994a, A&A 285, L25
Joncour I., Bertout C., Bouvier J., 1994b, A&A 291, L19
Kazarovets E.V. & Samus N.N., 1997, IBVS 4471
Knox K.T. & Thompson B.J., 1974, ApJ 193, L45
Kroupa P., 1995, MNRAS 277, 1507
Kürster M. & Schmitt J.H.M.M., 1996, A&A 311, 211
Kulkarni S.R., 1997, Science 276, 1350

Kurtz M.J., Mink D.J., Wyatt W.F., et al., 1992, In: Astronomical Data Analysis Software and Systems I. ASP Conf. Ser. 25, D.M. Worral, C. Biemesderfer, J. Barnes (Eds.), San Francisco, p. 432
Kurucz R.L., 1992a, In: The Stellar Population of Galaxies. IAU Symp. 149, B. Barbuy & A. Renzini (Eds.), Reidel, Dordrecht, p. 225
Kurucz R.L., 1992b, Rev. Mex. Astron. Astrofís. 23, 187
Kurucz R.L., 1993, *CD-ROM No. 18: ATLAS9 Stellar Atmospheres Programs and 2 km/s Grid*
Kurucz R.L., 1994, *CD-ROM No. 19: Solar Abundance Model Atmospheres for* $0, 1, 2, 4, 8\ km/s$
Kurucz R.L., Furenlid I., Brault J., Testerman L., 1984, *National Solar Observatory Atlas No. 1: Solar Flux Atlas from 296 to 1300 nm*. National Solar Observatory, Sunspot
Latham D.W., 1992, In: Complementary Approaches to Double and Multiple Star Research. IAU Coll. 135, ASP Conf. Ser. 32, H.A. McAlister & W. I. Hartkopf (Eds.) San Francisco, p. 110
Latham D.W., Nordström B., Andersen J., et al., 1996, A&A 314, 864
Leinert C., Henry T., Glindemann A., McCarthy D.W., 1997, A&A 325, 159
Lohmann A.W., Weigelt G., Wirnitzer B., 1983, Appl. Opt. 22, 4028
Maddalena R.J., Morris M., Moscowitz J., Thaddeus P., 1985, ApJ 303, 375
Marschall L.A. & Mathieu R.D., 1988, AJ 96, 1956
McCarthy J., Sandiford B., Boyd D., Booth J., 1993, PASP 105, 881
McNamara B., 1976, AJ 81, 375
McNamara B. & Huels S., 1983, AAS 54, 221
McNamara B., Hack W.J., Olson R.W., Mathieu R.D., 1989, AJ 97, 1427
Montes D., Fernandez-Figueroa M.J., de Castro E., et al., 1997, *The broad components in the* $H\alpha$ *line of very active stars: chromospheric microflaring ?*. In: Proc. of 10th Cambridge Workshop on 'Cool Stars, Stellar Systems, and the Sun'. PASP Conf. Proc. Ser., in press
Montmerle T., Koch-Miramond L., Falgarone E., Grindlay J.E., 1983, ApJ 269, 182
Morale F., Micela G., Favata F., Sciortino S., 1996, A&AS 119, 403
Neuhäuser R., 1997, Science 276, 1363
Neuhäuser R., Sterzik M.F., Schmitt J.H.M.M., Wichmann R., Krautter J., 1995a, A&A 297, 391
Neuhäuser R., Preibisch Th., Alcalá J.M., Schmitt J.H.M.M., 1995b, *Rotationally modulated X-ray emission on the young star P1724?*. In: K.G. Strassmeier (ed.) IAU Symposium 176 on 'Stellar Surface Structure'. Vienna, Austria, October 1995. Poster Proc. p. 197
Nordström B., Latham D.W., Morse J.A., et al., 1994, A&A 287, 338
Oláh K., Kõvári Zs., Bartus J., et al., 1997, A&A 321, 811
Palla F. & Stahler S., 1993, ApJ 418, 414
Parenago P.P., 1954, Trudy Gosud. Astron. Sternberga 25, 1
Pasquini L., 1993, Update to the ESO operating manual no. 2
Patterer R.J., Ramsey L., Huenemoerder D.P., Welty A.D., 1993, AJ 105, 1519
Pavlenko Ya P. & Magazzù A., 1996, A&A 311, 961
Penston M.V., Hunter J.K., O'Neill A., 1975, MNRAS 171, 219
Petrov P.P., Shcherbakov V.A., Berdyugina S.V., et al., 1994, A&AS 107, 9
Piskunov N.E., Kupka F., Ryabchikova T.A., Weiss W.W., Jeffery C.S., 1995, A&AS 112, 525
Preibisch Th., 1997, A&A 320, 525
Preibisch Th., Zinnecker H., Schmitt J.H.M.M., 1993, A&A 279, L33
Preibisch Th., Neuhäuser R., Alcalá J.M., 1995, A&A 304, L13
Press W.H. & Rybicki G.B., 1989, ApJ 338, 277
Rice J.B. & Strassmeier K.G., 1996, A&A 316, 164
Roberts D.H., Lehar J., Dreher J.W., 1987, AJ 93, 968
Röser S., 1996, IAU Symp. 172, 481
Röser S., Morrison J., et al., 1996, IAU Symp. 179
Schmitt J.H.M.M., Collura A., Sciortino S. et al., 1990, ApJ 365, 704
Schüssler M., Caligari P., Ferriz-Mas A., Solanki S.K., Stix M., 1996, A&A 314, 503
Soderblom D.R., Jones B.F., Balachandran S., et al., 1993, AJ 106, 1059
Stellingwerf R.F., 1978, ApJ 224, 953
Sterzik M.F. & Durisen R., 1995, A&A 304, L9
Sterzik M.F., Durisen R.H., Brandner W., Jurcevic J., Honeycutt R.K., 1997, AJ 114, 1555
Stout-Batalha N.M., 1997, PhD Thesis, University of California, Santa Cruz
Strand K.A., 1958, ApJ 128, 14
Strassmeier K.G., Welty A.D., Rice J.B., 1994, A&A 285, L17
Strassmeier K.G., Bartus J., Cutispoto G., Rodonó M., 1997, A&AS 125, 11
Strom K.M., Strom S.E., Edwards S., Cabrit S., Skrutskie M.F., 1989, AJ 97, 1451
Tagliaferri G., Cutispoto G., Pallavicini R., Randich S., Pasquini L., 1994, A&A 285, 272
Terranegra L., Chavarría C., Diaz S., Gonzales-Patino D., 1994, A&AS 104, 557
Tian K.P., van Leeuwen F., Zhao J.L., Su C.G., 1996, A&AS 118, 503
Tonry J. & Davis M., 1979, AJ 84, 1511
Trümper J., 1983, Adv. Space Res. 2, 241
Valenti J.A. & Piskunov N., 1996, A&AS 118, 595
Van Altena W.F., Lee J.T., Lee J.-F., Lu P.K., Upgren A.R., 1988, AJ 95, 1744
Vasilevskis S., 1971, ApJ 167, 537
Verschueren W. & Hensberge H., 1990, A&A 216, 216
Vogt S.S., Penrod G.D., Hatzes A.P., 1987, ApJ 341, 456
Vogt S.S. & Penrod G.D., 1983, PASP 95, 565
Walker M., 1969, ApJ 155, 447
Walter F.M., 1986, ApJ 306, 573
Warren W.H. & Hesser J.E., 1977, ApJS 34, 115
Weaver M.B. & Jones G., 1992, ApJS 78, 239
Welty A.D. & Ramsey L.W., 1995, AJ 110, 336
Wolk S.J., 1996, PhD Thesis, State University of New York at Stony Brook
Yamauchi S., Koyama K., Sakano M., Okada K., 1996, PASJ 48, 719
Zimmermann H.U., Becker W., Izzo C., et al., 1995, EXSAS Handbook, Garching